https://doi.org/10.1093/plphys/kiae098 PLANT PHYSIOLOGY 2024: 195: 2176–2194

Plant Physiology®

Research Article

Deletion of the sugar importer gene *OsSWEET1b* accelerates sugar starvation-promoted leaf senescence in rice

Dan Chen,[1,†] **Yarui Shi**,[1,†] **Peng Zhang**,[1] **Wenya Xie**,[1] **Shuxin Li**,[1] **Jinghua Xiao**,[1] **Meng Yuan**[1,*,‡]

1 National Key Laboratory of Crop Genetic Improvement, National Center of Plant Gene Research (Wuhan), Hubei Hongshan Laboratory, Huazhong Agricultural University, Wuhan 430070, China

*Author for correspondence: myuan@mail.hzau.edu.cn
†These authors contributed equally.
‡Senior author.
The author responsible for distribution of materials integral to the findings presented in this article in accordance with the policy described in the Instructions for Authors (https://academic.oup.com/plphys/pages/General-Instructions) is Meng Yuan (myuan@mail.hzau.edu.cn).

Abstract

Leaf senescence is a combined response of plant cells stimulated by internal and external signals. Sugars acting as signaling molecules or energy metabolites can influence the progression of leaf senescence. Both sugar starvation and accumulation can promote leaf senescence with diverse mechanisms that are reported in different species. Sugars Will Eventually be Exported Transporters (SWEETs) are proposed to play essential roles in sugar transport, but whether they have roles in senescence and the corresponding mechanism are unclear. Here, we functionally characterized a sugar transporter, OsSWEET1b, which transports sugar and promotes senescence in rice (*Oryza sativa* L.). OsSWEET1b could import glucose and galactose when heterologously expressed in *Xenopus* oocytes and translocate glucose and galactose from the extracellular apoplast into the intracellular cytosol in rice. Loss of function of *OsSWEET1b* decreased glucose and galactose accumulation in leaves. *ossweet1b* mutants showed accelerated leaf senescence under natural and dark-induced conditions. Exogenous application of glucose and galactose complemented the defect of *OsSWEET1b* deletion-promoted senescence. Moreover, the senescence-activated transcription factor OsWRKY53, acting as a transcriptional repressor, genetically functions upstream of *OsSWEET1b* to suppress its expression. *OsWRKY53*-overexpressing plants had attenuated sugar accumulation, exhibiting a similar phenotype as the *ossweet1b* mutants. Our findings demonstrate that OsWRKY53 downregulates *OsSWEET1b* to impair its influx transport activity, leading to compromised sugar accumulation in the cytosol of rice leaves where sugar starvation promotes leaf senescence.

Introduction

As the final stage of plant leaf development, leaf senescence is characterized by developmentally programed leaf yellowing (Woo et al. 2019). Leaf senescence is a combined response of leaf cells to internal developmental signals and external environmental signals. The major internal factors are hormonal and nutritional signals. Phytohormones including salicylic acid, ethylene, abscisic acid (ABA), jasmonic acid, brassinosteroid, and strigolactone function as senescence inducers, whereas auxin, cytokinin, and gibberellic acid (GA) act as senescence inhibitors (Woo et al. 2019). Nutrition such as sugars not only functions as primary signaling molecules but also

Received September 26, 2023. Accepted January 24, 2024. Advance access publication March 1, 2024.

Open Access

acts as essential cellular energy metabolites that can initiate and influence the progression of leaf senescence (Kim 2019).

Although sugars play critical roles in the regulation of leaf senescence, the effects of sugars on the modulation of senescence are debatable (van Doorn 2008; Asim et al. 2023). Some papers support that sugar starvation can induce or enhance leaf senescence which is supported by a series of evidence that either low sugar levels in leaf cells or prolonged dark treatment of detached leaves could accelerate senescence responses, while blocking sugar exportation from leaf cells or exogenous supply of sugars onto leaf disks could delay senescence responses (Li et al. 2020; Ni et al. 2020; Wu et al. 2023). Conversely, some papers show that sugar accumulation can promote leaf senescence which is backed by pieces of genetic or physiological evidence in some species (Zhou et al. 2014). The negative effects of sugar on the onset of leaf senescence are mainly evidenced by changes of the expression of senescence-associated genes (SAGs) and chlorophyll content or photosynthetic activity (Kim 2019). Moreover, the negative roles of sugar on leaf senescence regulation are mostly evident in dark-induced leaf senescence while rarely noticeable in sugar starvation-promoted leaf senescence (Li et al. 2020).

In general, sugars transported inside or outside of cells depend on sugar transporters. A class of sugar transporters named Sugars Will Eventually be Exported Transporters (SWEETs) which are conserved from archaebacteria to eukaryotes can facilitate the diffusion of sugar molecules across different cell membranes (Eom et al. 2015; Chen, Cheung, et al. 2015; Chen, Lin, et al. 2015). In plants, SWEETs play roles in multiple physiological processes including nutritional homeostasis (pollen, nectar, grain, and senescence), abiotic (cold, drought, heat, and salinity) stresses, and biotic (pathogen, insect) stresses (Eom et al. 2015; Chen, Cheung, et al. 2015; Chen, Lin, et al. 2015). SWEETs have been validated to function in remobilization of different sugars during plant senescence. In Arabidopsis (*Arabidopsis thaliana*), AtSWEET11, AtSWEET12, and AtSWEET15 act as sucrose exporters. The *atsweet11; 12* double mutant contained higher levels of sucrose (Chen et al. 2012), while the *AtSWEET11*, *AtSWEET12*, or *AtSWEET15* overexpression plants showed accelerated leaf senescence (Seo et al. 2011; Eom et al. 2015; Chen, Cheung, et al. 2015; Chen, Lin, et al. 2015). Rice (*Oryza sativa* L.) OsSWEET5 appeared to act as a galactose transporter when heterologously expressed in yeast. The *OsSWEET5*-overexpressing rice lines displayed precocious senescence and exhibited disordered sugar distribution with more contents of galactose, glucose, and fructose but less level of sucrose in leaves (Zhou et al. 2014). Similarly, the heterologous expression of pear (*Pyrus bretschneideri*) *PbSWEET4* in strawberry (*Fragaria vesca*) resulted in reduced leaf sugar contents and accelerated leaf senescence which might be caused by PbSWEET4-promoted sugar efflux from leaves (Ni et al. 2020). The maize (*Zea mays*) *zmsweet1b* knockout mutant had decreased sucrose and fructose contents and exhibited a senescence-like phenotype (Wu et al. 2023). Of the 21 *OsSWEET* members in rice, 6 of them showed a decreased expression pattern and 5 of them exhibited an increased expression pattern along with natural leaf senescence, indicating they might play roles in sugar-regulated senescence (Yuan et al. 2014). However, whether these OsSWEETs have transportation activity on sugars and their specific substrates toward different sugars, even the relationship between leaf senescence and OsSWEET-mediated sugar transportation, is largely unknown.

Several types of transcription factors including WRKY proteins have been reported to regulate leaf senescence by activating or repressing the transcription of their downstream genes (Woo et al. 2019; Wang et al. 2023). WRKYs positively or negatively regulate leaf senescence depending on their diverse target genes. In Arabidopsis, AtWRKY6, AtWRKY53, AtWRKY55, and AtWRKY71 can directly target and activate the expressions of receptor-like protein kinase genes, *senescence-induced receptor-like kinase* (*SIRK*) and *cysteine-rich receptor-like kinase 5* (*CRK5*), or SAGs, *senescence-associated gene 13* (*SAG13*), *senescence-associated gene 201* (*SAG201*), and *stay-green* (*SGR*), to positively influence senescence (Robatzek and Somssich 2002; Zhang et al. 2018; Wang et al. 2020; Yu et al. 2021; Burdiak et al. 2022). In rice, OsWRKY42 binds to the rice *Metallothionein 1d* (*OsMT1d*) promoter and represses its expression to promote senescence (Han et al. 2014). OsWRKY53 can directly target to the promoters of 2 ABA catabolic genes rice *ABA 8′-hydroxylase 1* (*OsABA8ox1*) and *OsABA8ox2* to repress their expressions, resulting in enhanced ABA accumulation which promotes leaf senescence (Xie et al. 2022). In general, WRKYs primarily regulate the expressions of SAGs or alter hormone homeostasis such as ABA to modulate senescence. However, whether WRKYs could regulate the expression of sugar transporters to alter sugar homeostasis in leaf cells to influence senescence is rarely reported.

It was previously reported that OsWRKY53 promotes leaf senescence by enhancing ABA-triggered hormonal signals; in this study, we supply evidence that OsWRKY53 modulates senescence by altering OsSWEET1b-mediated nutritional signals. We demonstrate that OsWRKY53 could directly bind to the promoter and repress the expression of *OsSWEET1b* which encodes a hexose transporter harboring influx transport activity for glucose and galactose. The compromised glucose and galactose accumulation in the *ossweet1b* mutant or the *OsWRKY53*-overexpressing plant accelerates leaf senescence. The revealed OsWRKY53-regulated *OsSWEET1b* regulatory network provides an additional module supporting the evidence that sugar starvation can enhance leaf senescence.

Results

The *ossweet1b* mutant shows accelerated leaf senescence

We previously generated individual homozygous knockout mutants for 19 rice *SWEET* genes (Li et al. 2022), of which the *ossweet1b* mutant showed obviously accelerated leaf

senescence at the heading stage and later on. To explore how *OsSWEET1b* regulates leaf senescence, we generated *OsSWEET1b*-overexpressing (*OsSWEET1b*-OE) transgenic plants in this study and evaluated leaf senescence of these transgenic plants. Transformation of rice with the *OsSWEET1b*-OE construct where the maize *Ubiquitin* promoter was used to regulate *OsSWEET1b* expression generated 10 independent *OsSWEET1b*-OE T_0 plants; RT-qPCR analyses showed that transcript levels of *OsSWEET1b* were significantly increased in these *OsSWEET1b*-OE transgenic plants (Supplementary Fig. S1).

We planted the *OsSWEET1b*-OE plants, *ossweet1b* mutants, and wild type (WT) in the paddy field to evaluate their leaf phenotypes by measuring Soil Plant Analysis Development (SPAD) and Fv/Fm values, ion leakage rate, and chlorophyll content in flag leaf at different growth stages. At the tillering stage, the *ossweet1b* mutant leaves were slightly yellow, while the *OsSWEET1b*-OE plants did not display noticeable phenotypic abnormalities compared with the WT (Fig. 1A; Supplementary Fig. S2). The *ossweet1b* mutants exhibited slightly lower SPAD and Fv/Fm values, higher ion leakage rates, and lower contents of chlorophyll a, chlorophyll b, and total chlorophyll than the WT, while the *OsSWEET1b*-OE plants had unchanged SPAD reading, Fv/Fm value, ion leakage rate, and chlorophyll contents relative to those of the WT (Fig. 1, B to E). At the heading stage, the *ossweet1b* mutant leaves were visibly yellow, especially the lower leaves were dark yellow, while the *OsSWEET1b*-OE plant leaves remained green (Fig. 1F; Supplementary Fig. S2). Accordingly, the *ossweet1b* mutants had decreased SPAD and Fv/Fm values, lower chlorophyll contents, and higher ion leakage rates, while the *OsSWEET1b*-OE plants had increased SPAD and Fv/Fm values, higher chlorophyll contents, and decreased ion leakage rates compared with those of the WT (Fig. 1, G to J). At the grain filling stage, the *ossweet1b* mutant leaves were totally yellow, while the *OsSWEET1b*-OE plant leaves remained green compared with slightly yellowish for WT leaves (Fig. 1K; Supplementary Fig. S2). In agreement, the *ossweet1b* mutants had 3.3-fold decreased SPAD reading, 1.8-fold decreased Fv/Fm value, 3.5-fold decreased chlorophyll a, 3.3-fold decreased chlorophyll b, 3.4-fold decreased total chlorophyll, and 2.7-fold increased ion leakage rate than the WT, while the *OsSWEET1b*-OE plants had 1.2-fold higher SPAD reading, 1.4-fold increased Fv/Fm value, 1.3-fold increased chlorophyll a, 1.4-fold increased chlorophyll b, 1.3-fold increased total chlorophyll, and 1.7-fold lower ion leakage rate than the WT (Fig. 1, L to O). From the tillering stage to grain filling stage, the *ossweet1b* mutant showed obviously accelerated leaf senescence supported by altered chlorophyll content, SPAD reading, Fv/Fm value, and ion leakage rate, while the *OsSWEET1b*-OE plant exhibited delayed leaf senescence, suggesting that *OsSWEET1b* is negatively involved in leaf senescence.

In order to validate that knocking out *OsSWEET1b* accelerates the leaf senescence, we kinetically analyzed the senescence symptoms of the transgenic rice plants from the seedling stage to the final senescence stage by measuring chlorophyll levels. There were similar chlorophyll levels between the *ossweet1b* mutants and WT at the seedling stage, while from the tillering stage to the senescence stage, the *ossweet1b* mutants had significantly decreased chlorophyll levels than the WT, and at the mature stage and senescence stage, chlorophyll levels in flag leaf of the *ossweet1b* mutants were almost undetected. Reversely, the *OsSWEET1b*-OE plants had higher chlorophyll contents than the WT in the flag leaf from the heading stage to the senescence stage (Supplementary Fig. S3). Although the *ossweet1b* mutants exhibited early senescence, they had similar heading dates as the WT and could undergo the whole process of growth and development (Supplementary Fig. S2). Therefore, we assume that the early senescence in the *ossweet1b* mutants is caused by functional loss of a senescence regulator but not developmental defect. Collectively, deletion of *OsSWEET1b* accelerates the leaf senescence.

Altered expression of genes involved in chlorophyll synthesis and degradation pathways

We investigated transcript levels of genes involved in chlorophyll synthesis and degradation pathways in flag leaf of the transgenic lines at the grain filling stage. Rice *Mg-chelatase D subunit* (*OsChlD*), *heme biosynthesis A* (*OsHemA*), and *3,8-divinyl(proto)chlorophyll(ide) α 8-vinyl reductase* (*OsDVR*), encoding key enzymes for chlorophyll biosynthesis in rice (Zhang et al. 2006; Wang et al. 2010; Zeng et al. 2020), had decreased expressions in the *ossweet1b* mutant but increased levels in the *OsSWEET1b*-OE plant relative to WT levels (Fig. 2A). Reversely, rice *red chlorophyll catabolite reductase 1* (*OsRCCR1*), *nonyellow coloring 1* (*OsNYC1*), and *stay-green* (*OsSGR*), playing essential roles in chlorophyll degradation in rice (Jiang et al. 2007; Sato et al. 2009; Tang et al. 2011), had significantly enhanced expressions in the *ossweet1b* mutant but compromised transcriptions in the *OsSWEET1b*-OE plant than in the WT (Fig. 2B). Enhanced expression of genes associated with chlorophyll degradation and attenuated expression of chlorophyll biosynthesis-related genes in the *ossweet1b* mutant support accelerated leaf senescence for the mutant.

Altered expression of SAGs

We simultaneously investigated transcript level of representative SAGs in flag leaf of the transgenic lines at the grain filling stage. Rice *delay of the onset of senescence* (*OsDOS*), *senescence-related indicator 57* (*OsI57*), and *senescence-related indicator 85* (*OsI85*) are marker SAGs of leaf senescence. OsDOS negatively regulates leaf senescence (Kong et al. 2006). *OsI57* and *OsI85* expressions are induced during leaf senescence (Lee et al. 2001). RT-qPCR assays showed that both *OsI57* and *OsI85* had obviously enhanced expressions in the *ossweet1b* mutant while decreased expressions in the *OsSWEET1b*-OE plant than in the WT. *OsDOS*

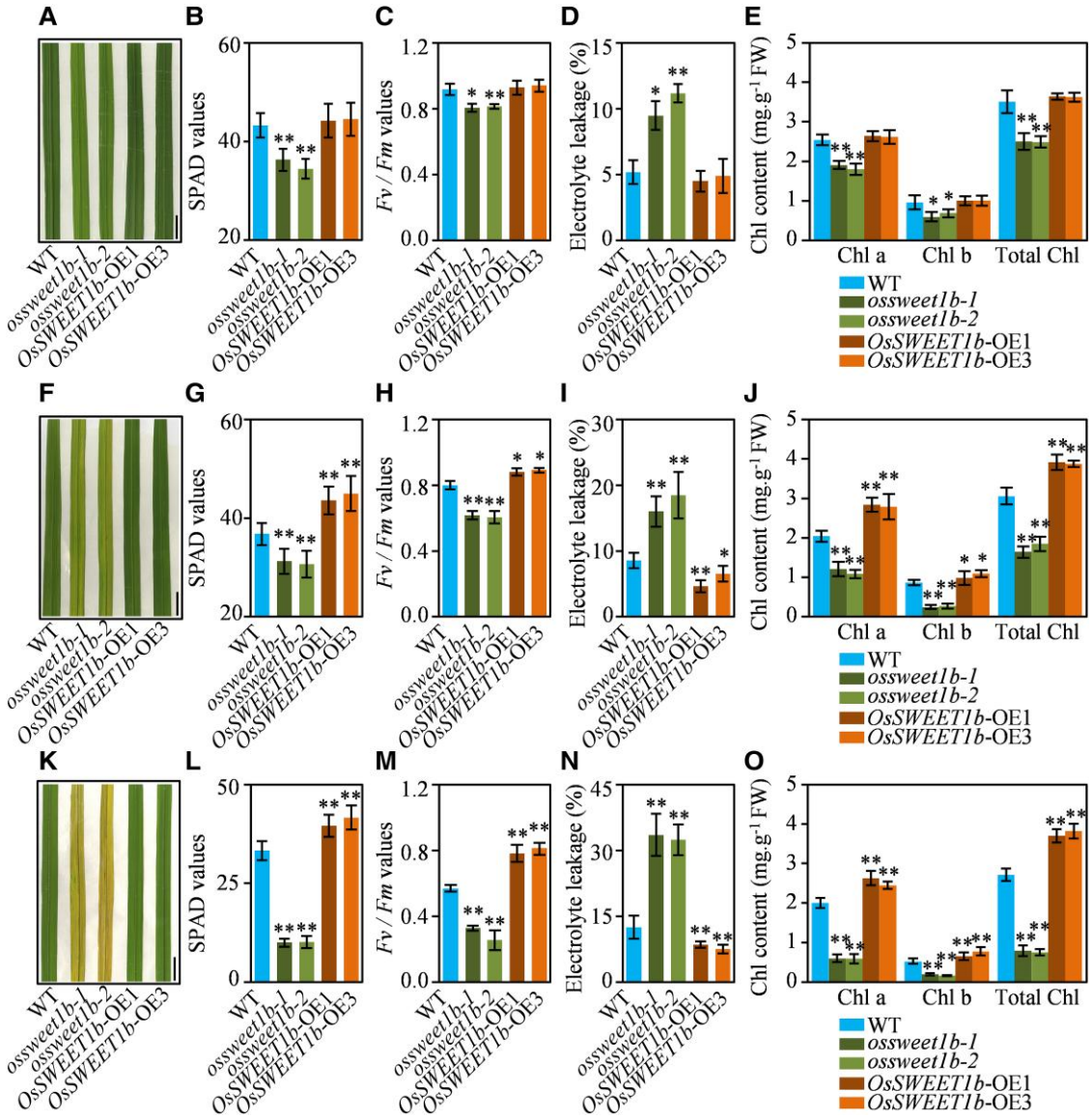

Figure 1. The *ossweet1b* mutant shows accelerated leaf senescence. **A)** Senescing flag leaf of *OsSWEET1b*-OE, *ossweet1b*, and WT at the tillering stage. **B)** SPAD values of flag leaf of *OsSWEET1b*-OE, *ossweet1b*, and WT at the tillering stage. **C)** Fv/Fm values of flag leaf of *OsSWEET1b*-OE, *ossweet1b*, and WT at the tillering stage. **D)** Electrolyte leakage analysis of flag leaf of *OsSWEET1b*-OE, *ossweet1b*, and WT at the tillering stage. **E)** Chlorophyll contents of flag leaf of *OsSWEET1b*-OE, *ossweet1b*, and WT at the tillering stage. **F)** Senescing flag leaf of *OsSWEET1b*-OE, *ossweet1b*, and WT at the heading stage. **G)** SPAD values of flag leaf of *OsSWEET1b*-OE, *ossweet1b*, and WT at the heading stage. **H)** Fv/Fm values of flag leaf of *OsSWEET1b*-OE, *ossweet1b*, and WT at the heading stage. **I)** Electrolyte leakage analysis of flag leaf of *OsSWEET1b*-OE, *ossweet1b*, and WT at the heading stage. **J)** Chlorophyll contents of flag leaf of *OsSWEET1b*-OE, *ossweet1b*, and WT at the heading stage. **K)** Senescing flag leaf of *OsSWEET1b*-OE, *ossweet1b*, and WT at the grain filling stage. **L)** SPAD values of flag leaf of *OsSWEET1b*-OE, *ossweet1b*, and WT at the grain filling stage. **M)** Fv/Fm values of flag leaf of *OsSWEET1b*-OE, *ossweet1b*, and WT at the grain filling stage. **N)** Electrolyte leakage analysis of flag leaf of *OsSWEET1b*-OE, *ossweet1b*, and WT at the grain filling stage. **O)** Chlorophyll contents of flag leaf of *OsSWEET1b*-OE, *ossweet1b*, and WT at the grain filling stage. Scale bars: 1 cm. Data represent mean ± SD; $n = 30$ includes 3 biological replicates and 10 technical replicates for each biological replicate in **B)**, **C)**, **D)**, **G)**, **H)**, **I)**, **L)**, **M)**, and **N)**. Data represent mean ± SE; $n = 3$ biological replicates in **E)**, **J)**, and **O)**. Asterisks in **B)**, **C)**, **D)**, **E)**, **G)**, **H)**, **I)**, **J)**, **L)**, **M)**, **N)**, and **O)** indicate a significant difference between transgenic plants and WT as determined by 2-tailed Student's *t* test at $^{**}P < 0.01$ or $^{*}P < 0.05$.

had reverse expressional pattern compared with *OsI57* or *OsI85* in the transgenic plants (Fig. 2C). Taken together, the altered expression of marker SAGs further supports that the early senescence in the *ossweet1b* mutants is caused by functional loss of a senescence regulator.

Abnormal ROS accumulation in the *ossweet1b* mutant

Since ROS generation is one of the earliest responses of plant cells under senescence, we speculated that the *ossweet1b* mutant may have altered ROS accumulation. To confirm

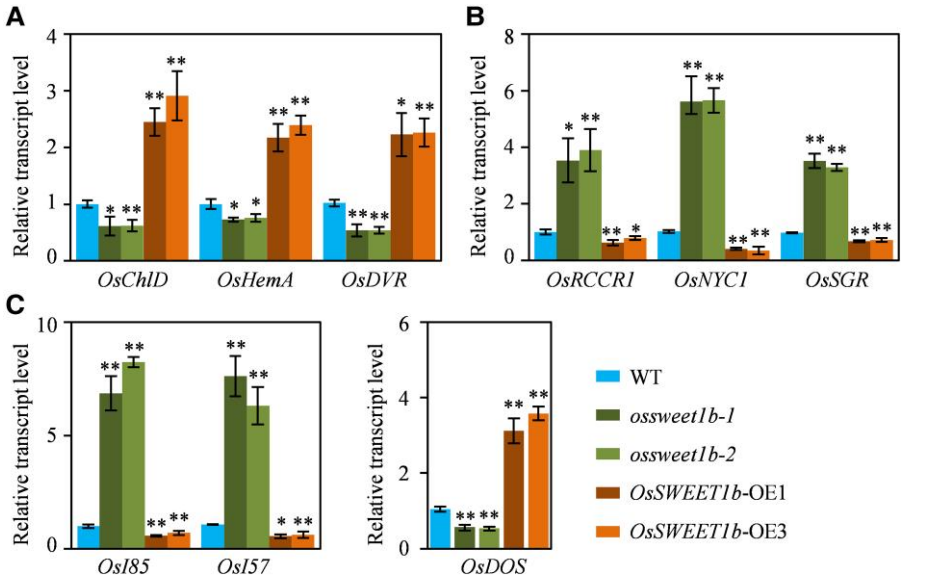

Figure 2. Transcript levels of representative chlorophyll synthesis genes, chlorophyll degradation genes, and SAGs in flag leaf at the grain filling stage. **A)** Transcript levels of chlorophyll synthesis genes. **B)** Transcript levels of chlorophyll degradation genes. **C)** Transcript levels of SAGs. Data represent mean ± SE for 3 biological replicates. Gene expression analysis was performed by RT-qPCR and normalized to *Actin*. Asterisks in **A)**, **B)**, and **C)** indicate a significant difference between transgenic plants and WT as determined by 2-tailed Student's *t* test at $^{**}P < 0.01$ or $^{*}P < 0.05$.

our hypothesis, we stained flag leaf of the *ossweet1b* mutant, *OsSWEET1b*-OE plant, and WT with 3,3′-diaminobenzidine (DAB), a dye that has been widely used to indicate H_2O_2 accumulation. DAB staining showed that obvious red-brown precipitates were exclusively found in the *ossweet1b* mutant leaves, while no such precipitates were observed in the *OsSWEET1b*-OE plant or WT leaves (Fig. 3A). In agreement, there were 1.5- to 1.7-fold higher H_2O_2 contents in the *ossweet1b* mutant flag leaf than that of the WT, while the *OsSWEET1b*-OE plant had slightly decreased H_2O_2 content (Fig. 3B).

H_2O_2 accumulation is usually associated with disrupted ROS scavenging system in plants. To confirm the possibility, we measured activities of superoxide dismutase (SOD) and peroxidase (POD), 2 primary antioxidative enzymes, in flag leaf of these plants. Results showed that the *ossweet1b* mutant had significantly higher SOD and POD activities, while the *OsSWEET1b*-OE plant had slightly lower SOD and POD activities than the WT (Fig. 3, C and D). Moreover, we measured the accumulation of malondialdehyde (MDA) which indirectly reflects the changes of cell damage. Notably, the *ossweet1b* mutant had ∼2-fold higher MDA content, while the *OsSWEET1b*-OE plant had 1.2-fold lower MDA level than that of the WT (Fig. 3E). Collectively, the abnormal ROS accumulation in the *ossweet1b* mutant additionally suggests that knockout of *OsSWEET1b* accelerates rice leaf senescence.

Knockout of *OsSWEET1b* promotes dark-induced senescence

To further explore accelerated leaf senescence by knockout of *OsSWEET1b* in more detail, we evaluated the responses of transgenic plants under dark treatment. Detached leaf discs from *OsSWEET1b*-OE, *ossweet1b*, and WT plants were floated on MES solution and incubated in the dark to mimic dark-induced senescence. After 5 d of dark incubation (DDI), the *ossweet1b* leaf discs were yellowish, while *OsSWEET1b*-OE leaf discs remained green compared with light green of WT leaf discs (Supplementary Fig. S4A). Consistent with yellowing leaves, lower chlorophyll contents were observed for the *ossweet1b* mutant, while higher chlorophyll levels were determined for the *OsSWEET1b*-OE plant than the WT (Supplementary Fig. S4B), indicating that knockout of *OsSWEET1b* promotes dark-induced senescence.

Expression pattern of *OsSWEET1b*

The expression pattern of *OsSWEET1b* was investigated in different tissues throughout the growth period of rice planted in paddy fields. *OsSWEET1b* was constitutively expressed in all tissues examined (Supplementary Fig. S5A). From the vegetative growth stages including 3-wk-old seedling, the tillering and the booting stages, to the reproductive stages including the heading and grain filling stages, *OsSWEET1b* showed a substantially higher expression in leaves and sheaths than in other tissues. Moreover, the expressions of *OsSWEET1b* in leaves and sheaths were higher at the reproductive stages than at the vegetative growth stages. Simultaneously, we tested *OsSWEET1b* expression in leaves under natural senescence. *OsSWEET1b* transcripts decreased gradually along with rice leaf senescence (Supplementary Fig. S5B). In addition, we assessed *OsSWEET1b* expressions under biotic and abiotic stress treatments. *OsSWEET1b* did not respond to bacterial pathogens and fungal pathogen infection (Supplementary Fig. S5C), and also to drought and salt

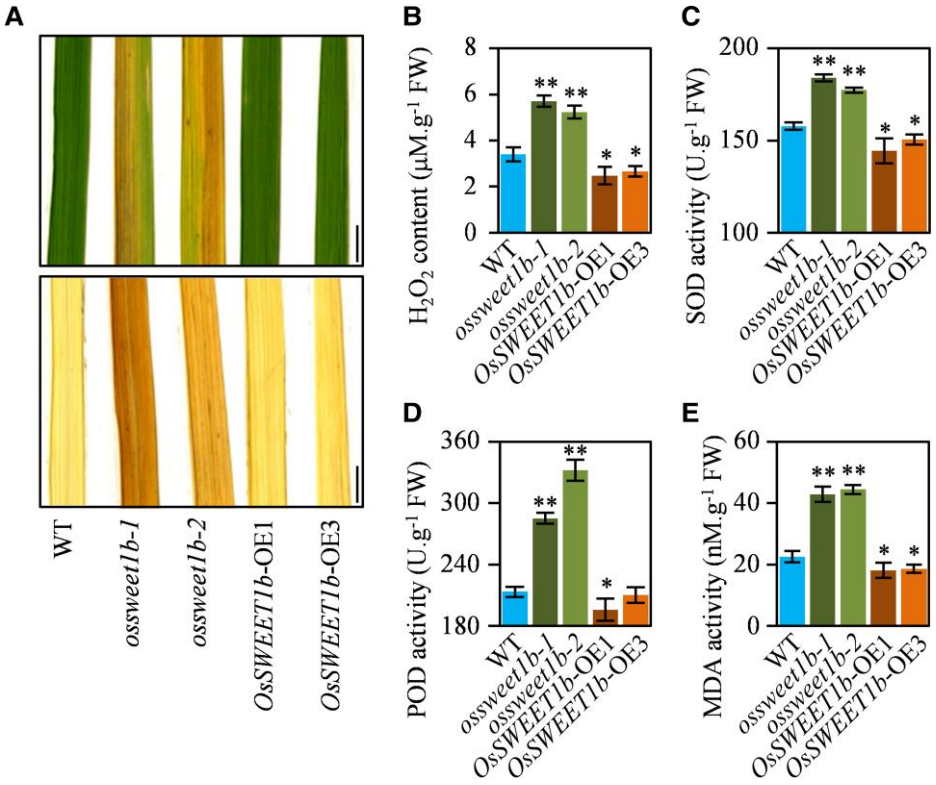

Figure 3. Impaired ROS homeostasis in the *ossweet1b* mutants. **A)** DAB staining for the *OsSWEET1b*-OE plants, *ossweet1b* mutants, and WT flag leaf. Scale bars: 1 cm. **B)** H_2O_2 levels in the transgenic rice plants and WT flag leaf. **C)** SOD activity in the transgenic rice plants and WT flag leaf. **D)** POD activity in the transgenic rice plants and WT flag leaf. **E)** MDA activity in the transgenic rice plants and WT flag leaf. Data represent mean ± SE of 3 biological replicates. Asterisks in **B)**, **C)**, **D)**, and **E)** indicate a significant difference between transgenic plants and WT as determined by 2-tailed Student's *t* test at $^{**}P < 0.01$ or $^{*}P < 0.05$.

treatments (Supplementary Fig. S5D), while had slightly increased expression after cold treatments.

OsSWEET1b was predicted to localize to the plasma membrane, which was confirmed by transient transfection of the OsSWEET1b:GFP construct encoding a fusion between *OsSWEET1b* and the GFP into rice protoplasts. OsSWEET1b:GFP exclusively colocalized with secretory carrier membrane protein (SCAMP1) which was fused to the red fluorescent protein (RFP) as a plasma membrane-localized marker protein (Fig. 4A), suggesting OsSWEET1b is a plasma membrane protein.

OsSWEET1b is a hexose importer

SWEET family proteins transport various sugars across membranes (Eom et al. 2015; Chen, Cheung, et al. 2015; Chen, Lin, et al. 2015). OsSWEET1b was previously predicted functioning as a hexose transporter because it can rescue the growth of yeast mutant EBY.VW4000 which lacks sugar uptake ability in the medium supplemented with galactose (Yuan et al. 2014; Tao et al. 2015). Here, *OsSWEET1b* transcript increased after galactose treatment (Supplementary Fig. S5E), suggesting OsSWEET1b might be involved in sugar transportation. To determine the influx transport activity of OsSWEET1b for glucose, galactose, and sucrose, complementary RNAs (cRNAs) of *OsSWEET1b*, *OsSWEET14* (serving as a positive control of influx transporter for glucose and sucrose; Chen et al. 2012), Arabidopsis *AtSWEET5* (serving as a positive control of influx transporter for galactose; Wang et al. 2022), or water (serving as a negative control) were injected into *Xenopus* oocytes. The oocytes were exposed to ^{14}C-labeled sugar ([^{14}C]glucose, [^{14}C]sucrose, or [^{14}C]galactose), and the radioactivity in the oocytes was determined. OsSWEET1b showed influx activity for glucose and galactose but not for sucrose (Fig. 4B). A kinetic analysis showed that the K_m values of OsSWEET1b for glucose and galactose uptake were 147 ± 29 and $2{,}073 \pm 408$ mM, respectively (Fig. 4C).

To determine whether OsSWEET1b has efflux transport activity, cRNAs of *OsSWEET1b*, *OsSWEET14* (serving as a positive control of efflux transporter for glucose; Chen et al. 2012), *OsSWEET11* (serving as a positive control of efflux transporter for sucrose; Chen et al. 2012), or water (serving as a negative control) were injected into *Xenopus* oocytes, and then, efflux activities were detected by monitoring time-dependent release of [^{14}C]glucose, [^{14}C]sucrose, or [^{14}C]galactose from oocytes after injection of the ^{14}C-labeled sugars and were expressed as percentage (sugar effluxed/total sugar injected × 100) to normalize the variations in injection, oocyte size, or cellular status. Results revealed that OsSWEET1b did not show efflux transport

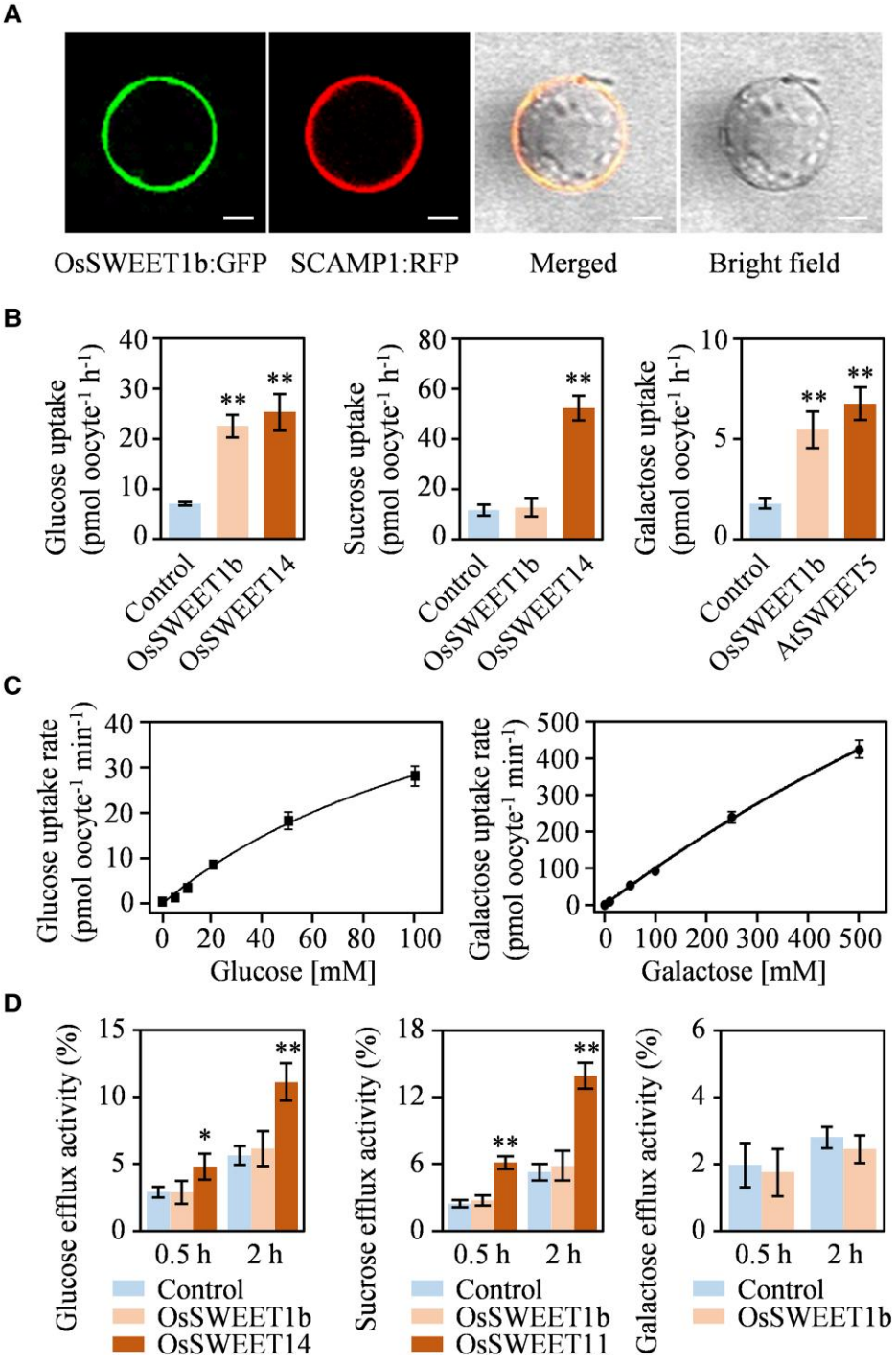

Figure 4. Sugar transporter activity of OsSWEET1b. **A)** Subcellular localization of OsSWEET1b:GFP in rice protoplasts. SCAMP1:RFP is used as a plasma membrane-localized marker protein. Scale bars: 10 μm. **B)** Uptake of glucose, sucrose, and galactose from *Xenopus* oocytes. **C)** Kinetics of OsSWEET1b for glucose and galactose uptake in *Xenopus* oocytes. **D)** Efflux of glucose, sucrose, and galactose from *Xenopus* oocytes. Data represent mean ± SD of 8 biological replicates. Asterisks in **B)** and **D)** indicate a significant difference between control and SWEET protein as determined by 2-tailed Student's *t* test at $^{**}P < 0.01$ or $^{*}P < 0.05$.

activity for glucose, galactose, and sucrose (Fig. 4D). Collectively, these results indicate that OsSWEET1b is a hexose transporter harboring influx transport activity for glucose and galactose.

Attenuated sugar contents in the *ossweet1b* mutant

To investigate the uptake activity of OsSWEET1b for sugar in planta, we measured contents of glucose, fructose, galactose, mannose, and sucrose in the flag leaf of these transgenic plants

at different growth stages. From the tillering stage to grain filling stage, there were significantly higher glucose and galactose contents in the *OsSWEET1b*-OE plant but obviously lower levels of these 2 sugars in the *ossweet1b* mutant than the WT. However, comparable contents of fructose, mannose, and sucrose were observed between in the *OsSWEET1b*-OE plant or *ossweet1b* mutant and WT (Fig. 5A). In plants, glucose is largely converted into starch which is stored as energy. In line with higher glucose content in the *OsSWEET1b*-OE plant, we found the *OsSWEET1b*-OE flag leaf accumulated more starch at different growth stages than the WT. In contrast, the *ossweet1b* mutant flag leaf had less starch relative to WT (Supplementary Fig. S6A). Moreover, rice ADP-glucose pyrophosphorylase-encoding genes *OsAGPS1* encoding the small catalytic subunit and *OsAGPL1* and *OsAGPL3* encoding the larger regulatory subunits of rice AGPase which is a key enzyme for starch synthesis (Ohdan et al. 2005) had significantly lower expressions in the *ossweet1b* mutant flag leaf while higher expressions in the *OsSWEET1b*-OE flag leaf than the WT at the grain filling stage (Supplementary Fig. S6B). These results suggest that OsSWEET1b is involved in glucose and galactose import in planta.

SWEET transporters on the plasma membrane facilitate sugar allocation (Eom et al. 2015; Chen, Cheung, et al. 2015; Chen, Lin, et al. 2015; Xue et al. 2022). OsSWEET1b acts as a plasma membrane-localized transporter and could import glucose and galactose. The above results reminded us that OsSWEET1b may translocate sugars from the extracellular apoplast into the intracellular cytosol. To test the possibility, we collected apoplastic fluid using the well-established infiltration–centrifugation method to assess apoplastic sugar content (Nouchi et al. 2012). Along with rice growing, highly silicified leaves make infiltration and apoplastic fluid collection challenging. Because of this, we used 3-wk-old seedling leaves to measure apoplastic sugar content. We found there were 1.6-fold higher glucose and 1.8-fold higher galactose in the apoplast of the *ossweet1b* mutant while 1.8-fold lower glucose and 1.4-fold lower galactose in the apoplast of the *OsSWEET1b*-OE plant relative to those in the WT apoplast. However, there were comparable contents of fructose, mannose, and sucrose in the apoplast of these plants (Fig. 5B). In addition, we measured sugar levels in the protoplast to indirectly evaluate sugar contents in cytosol. The were 1.9-fold less glucose and 1.7-fold less galactose in the protoplast of the *ossweet1b* mutant and 1.5-fold more glucose and 1.7-fold more galactose in the protoplast of the *OsSWEET1b*-OE plant than those in the WT protoplast. In contrast, there were comparable contents of fructose, mannose, and sucrose in the protoplast of these plants (Fig. 5C). Together, these results provide functional evidence that OsSWEET1b can translocate sugars like glucose and galactose from the extracellular apoplast into the intracellular cytosol.

Exogenous application of sugar delays the accelerated leaf senescence of *ossweet1b* mutant

To confirm whether the accelerated leaf senescence of the *ossweet1b* mutant was sugar dependent, we analyzed the response of the *ossweet1b* mutant to exogenous application of sugar under dark treatment. Detached leaf discs from the *ossweet1b* mutant and WT plants were floated on MES solution containing different sugars and incubated in the dark to mimic dark-induced senescence, with treatment without exogenous application of sugars as control. After dark incubation, the *ossweet1b* leaf discs were severely yellow (Fig. 6, A and D), accompanied by markedly decreased chlorophyll contents (Fig. 6, B and E), enhanced expression of *OsI57*, and attenuated expression of *OsDOS* than the WT (Fig. 6, C and F). Exogenous applications of glucose and galactose could substantially delay the senescence under dark treatment in the *ossweet1b* mutant and WT, as evidenced by the higher chlorophyll contents compared with mock-treated plants. However, both glucose and galactose application could retard the senescence of the *ossweet1b* mutant that the mutant even showed higher chlorophyll contents than mock-treated WT (Fig. 6, B and E). In agreement, the *ossweet1b* mutant had lower expression of *OsI57* and higher expression of *OsDOS* after treatment of glucose or galactose than mock-treated WT (Fig. 6, C and F). Moreover, although exogenous applications of sucrose and fructose could delay the senescence under dark treatment in the *ossweet1b* mutant and WT, the increased chlorophyll contents were comparable in both the *ossweet1b* mutant and WT (Supplementary Fig. S7). Taken together, these results support the inference that accelerated leaf senescence of the *ossweet1b* mutant is due to the shortage of glucose or galactose.

OsWRKY53 directly represses *OsSWEET1b* transcription

To mine genetically upstream transcription factors that directly regulate *OsSWEET1b* transcription, the yeast 1-hybrid assay was performed using a 2 kb *OsSWEET1b* promoter and rice leaf-derived cDNA library. Yeast 1-hybrid assay showed that several transcription factors could bind to *OsSWEET1b* promoter (Supplementary Table S1), of which OsWRKY53, acting as a positive regulator of leaf senescence (Xie et al. 2022), was selected for further analysis in this study. In previous studies, the *OsWRKY53*-overexpressing plant showed accelerated leaf senescence and the *oswrky53* knockout mutant exhibited delayed leaf senescence (Tian et al. 2017; Xie et al. 2022). OsWRKY53 functions as a transcription repressor by binding to the canonical W-box with TTGACC core sequence of its downstream target genes (Xie et al. 2021). Notably, the 2 kb *OsSWEET1b* promoter contains 3 putative W-box motifs which might be the OsWRKY53 binding sequence. To confirm *OsSWEET1b* is the target gene of OsWRKY53, we conducted a series of assays. Firstly, we tested *OsWRKY53* expression in leaves under natural senescence. *OsWRKY53* transcript levels increased gradually along with rice leaf senescence, showing an opposite pattern compared with *OsSWEET1b* (Supplementary Fig. S5B). We also evaluated *OsWRKY53* expression under sugar treatment, with the result that *OsWRKY53* transcript levels increased slightly but decreased soon after galactose treatment,

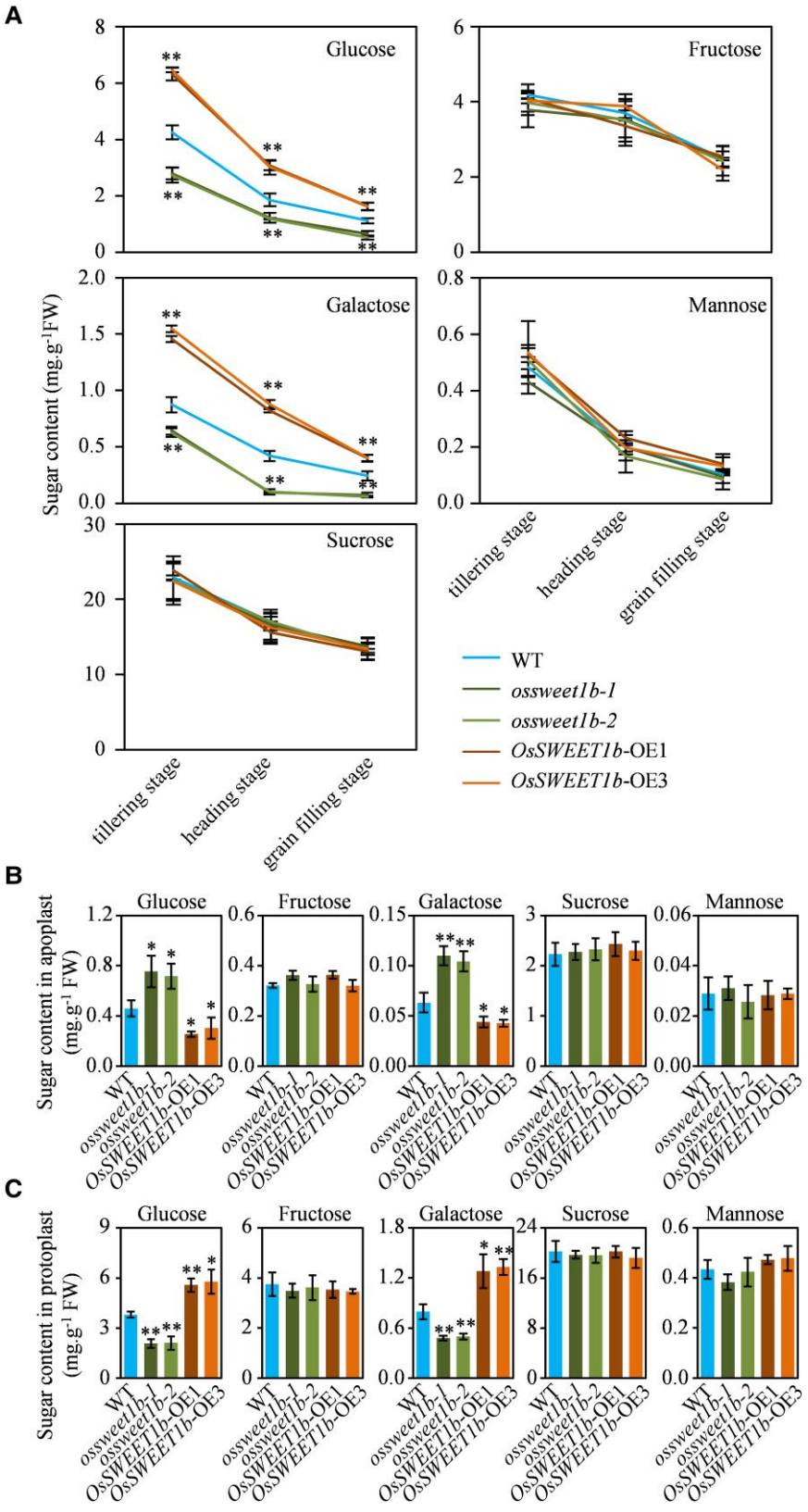

Figure 5. Sugar contents in leaves of the *ossweet1b* mutant and *OsSWEET1b*-OE plant. **A)** Sugar contents in the transgenic rice plants and WT flag leaf at the different growth stages. **B)** Apoplastic sugar contents in the transgenic rice plants and WT at 3-wk-old seedling stage. **C)** Sugar contents in protoplasts of the transgenic rice plants and WT at 3-wk-old seedling stage. Data represent mean ± SE of 3 biological replicates. Asterisks in **A)**, **B)**, and **C)** indicate a significant difference between transgenic plants and WT as determined by 2-tailed Student's *t* test at $^{**}P < 0.01$ or $^{*}P < 0.05$.

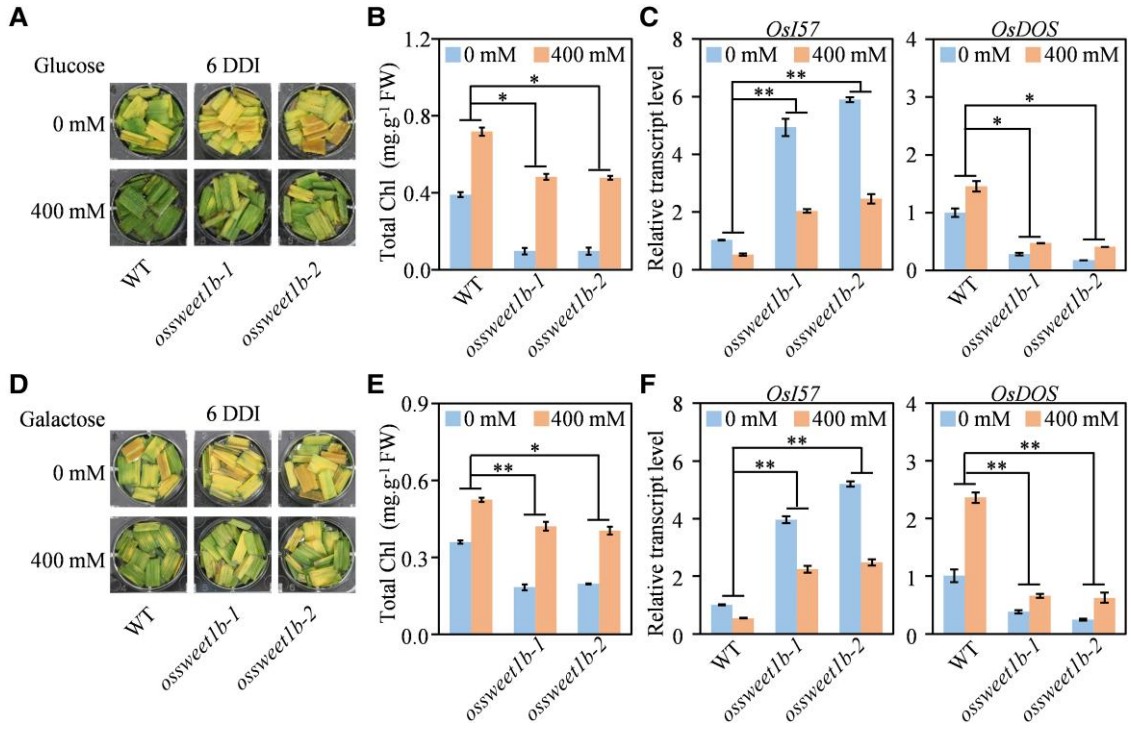

Figure 6. Exogenous applications of glucose and galactose delay the accelerated leaf senescence of *ossweet1b* mutant. **A)** Phenotype of detached leaf of *ossweet1b* and WT after dark treatment with or without additional glucose. DDI, day of dark incubation. **B)** Total chlorophyll content of *ossweet1b* and WT after dark treatment with or without additional glucose. **C)** Relative transcript levels of *OsI57* and *OsDOS* in detached leaf of *ossweet1b* and WT after dark treatment with or without additional glucose. **D)** Phenotype of detached leaf of *ossweet1b* and WT after dark treatment with or without additional galactose. **E)** Total chlorophyll content of *ossweet1b* and WT after dark treatment with or without additional galactose. **F)** Relative transcript levels of *OsI57* and *OsDOS* in detached leaf of *ossweet1b* and WT after dark treatment with or without additional galactose. Data represent mean ± SE of 3 biological replicates. Gene expression analysis was performed by RT-qPCR and normalized to *Actin*. Statistical significance was determined through 2-way ANOVA with Tukey's multiple comparisons test at $^{**}P < 0.01$ or $^{*}P < 0.05$.

while its expression did not respond to glucose treatment (Supplementary Fig. S5E). Simultaneously, we detected *OsSWEET1b* transcription in the flag leaf of *OsWRKY53* transgenic plants. RT-qPCR results showed that *OsSWEET1b* had significantly decreased expression in the *OsWRKY53*-OE plant while increased expression in the *oswrky53* mutant than the WT (Fig. 7A). Then, to determine the direct interaction between OsWRKY53 and promoter of *OsSWEET1b*, we employed electrophoretic mobility shift assays (EMSAs) to test the direct binding of OsWRKY53 to the W-box motif in vitro. A prokaryote-expressed and purified recombinant fusion protein consisting of His-TF and OsWRKY53 efficiently bound to W-box motif-containing probes but not mutated probes (Fig. 7B). Equal amounts of unlabeled and mutated W-box motif-containing probes could not efficiently impair the binding activity of OsWRKY53 on labeled W-box motif, while increasing amounts of unlabeled probes could weaken OsWRKY53 binding on labeled W-box motif (Supplementary Fig. S8). These EMSAs suggest that OsWRKY53 specifically binds to W-box motif within the *OsSWEET1b* promoter (Fig. 7B). Moreover, we performed chromatin immunoprecipitation (ChIP)-qPCR assays to test the binding of OsWRKY53 to these W-box motifs within the *OsSWEET1b* promoter in vivo. OsWRKY53 binding was enriched at the 2 W-box motifs (−1,048∼−1,043 and −194∼−189 bp) near the translational ATG start codon while not enriched at the third W-box (−1,733∼−1,728 bp) far away from the ATG in the *OsSWEET1b* promoter (Fig. 7C), suggesting OsWRKY53 bound to the *OsSWEET1b* promoter in vivo. In addition, to determine the effect of OsWRKY53 on the *OsSWEET1b* expression, we performed transient expression assays in rice protoplast cells using a construct in which *OsWRKY53* is driven by the *Ubiquitin* promoter as an effector and a construct in which the firefly luciferase (LUC) gene is driven by the intact or mutated *OsSWEET1b* promoter as a reporter. The $P_{OsSWEET1b}$:LUC construct but not the m$P_{OsSWEET1b}$:LUC construct resulted in significantly decreased LUC activity in protoplasts, confirming transcriptional repression for OsWRKY53 on *OsSWEET1b* (Fig. 7D). Collectively, these results indicate that OsWRKY53 can directly bind to the promoter of *OsSWEET1b* to suppress its transcription.

OsWRKY53 genetically acts upstream of *OsSWEET1b*

To assess the genetic epistasis between *OsWRKY53* and *OsSWEET1b* in the regulation of senescence, we knocked out *OsSWEET1b* in the *oswrky53* mutant to evaluate leaf phenotype of the *oswrky53 ossweet1b* double mutant (Supplementary Fig. S9). Compared with delayed leaf

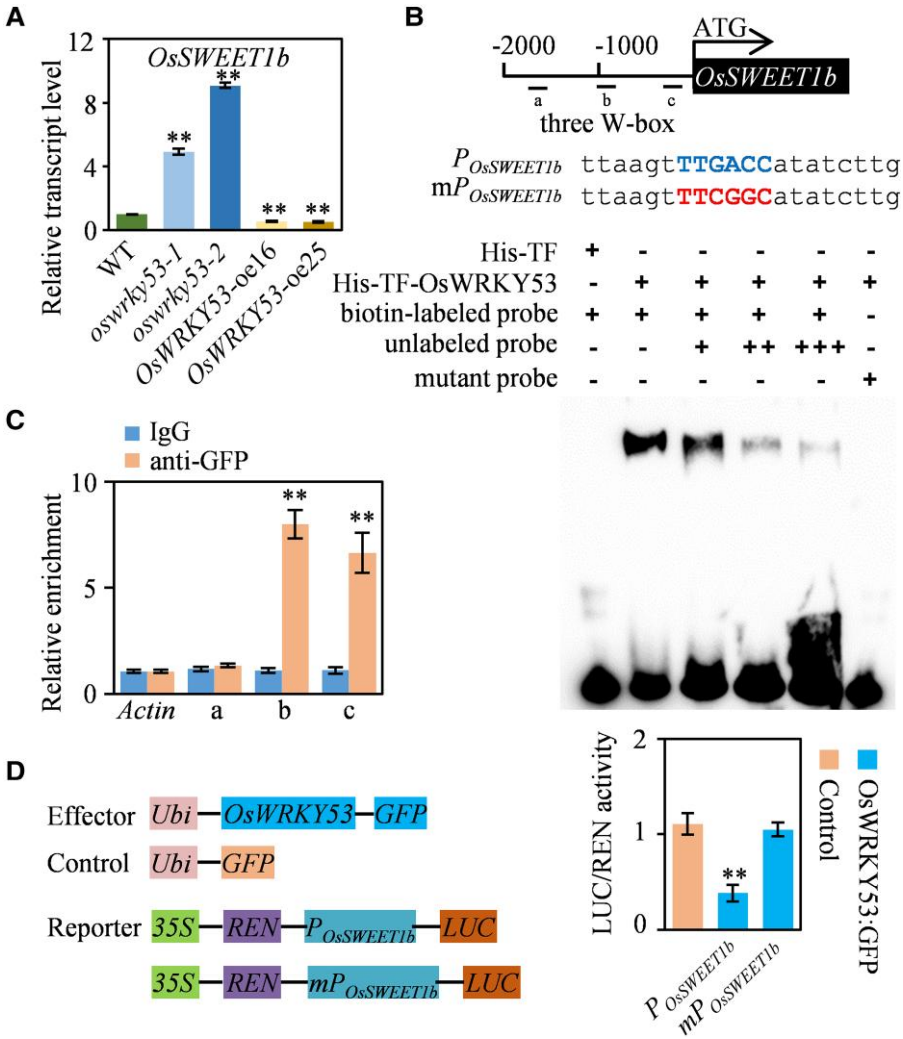

Figure 7. OsWRKY53 binds to *OsSWEET1b* promoter and suppresses *OsSWEET1b* transcription. **A)** *OsSWEET1b* expression in *OsWRKY53*-OE, *oswrky53* mutants, and WT. **B)** DNA binding activity assay of OsWRKY53 by EMSA. The blue capital letters indicate the intact W-box, and the red capital letters represent the mutated W-box. **C)** Binding assay of OsWRKY53 to the promoter of *OsSWEET1b* by ChIP-qPCR in *OsWRKY53*:GFP plants using the anti-GFP antibody. Anti-GFP antibody was used for immunoprecipitation and IgG acted as a control. **D)** Activity assay of OsWRKY53 in regulating *OsSWEET1b* expression. Data represent mean ± SE of 3 biological replicates. Gene expression analysis was performed by RT-qPCR and normalized to *Actin*. Asterisks in **A)** and **C)** indicate a significant difference between transgenic plants and WT as determined by 2-tailed Student's *t* test at $^{**}P < 0.01$ or in **D)** indicate a significant difference between control and reporter determined by 2-tailed Student's *t* test at $^{**}P < 0.01$.

senescence of the *oswrky53* knockout mutant, the *oswrky53 ossweet1b* double mutants exhibited accelerated leaf senescence, copying the *ossweet1b* mutant (Fig. 8A). In line with delayed leaf senescence, the *oswrky53* mutant had higher SPAD reading, Fv/Fm value, and chlorophyll content and lower ion leakage rate in flag leaf than that of the WT. Reversely, the *oswrky53 ossweet1b* double mutants had decreased SPAD reading, Fv/Fm value, and chlorophyll content and increased ion leakage rate in flag leaf relative to that of the WT. Moreover, the *oswrky53 ossweet1b* double mutants had comparable parameters of senescence as the *ossweet1b* mutant (Fig. 8, B to E).

Simultaneously, we assessed contents of glucose and galactose in the flag leaf of the *oswrky53* single mutant and *oswrky53 ossweet1b* double mutant at different growth stages. From the tillering stage to the grain filling stage, both glucose and galactose contents decreased in all the investigated rice lines. However, the *oswrky53* mutant had markedly higher and the *oswrky53 ossweet1b* double mutant had obviously lower glucose and galactose contents relative to them in the WT at the same growth stage (Fig. 8F). Moreover, the *oswrky53* single mutant had lower glucose and galactose contents in the apoplast but more of them in the protoplast relative to WT. Reversely, the *oswrky53 ossweet1b* double mutant accumulated higher glucose and galactose levels in the apoplast but less of them in the protoplast compared with WT or the *oswrky53* mutant (Fig. 8, G and H).

In addition, we measured different sugar contents in the flag leaf of the *OsWRKY53* transgenic plants at different

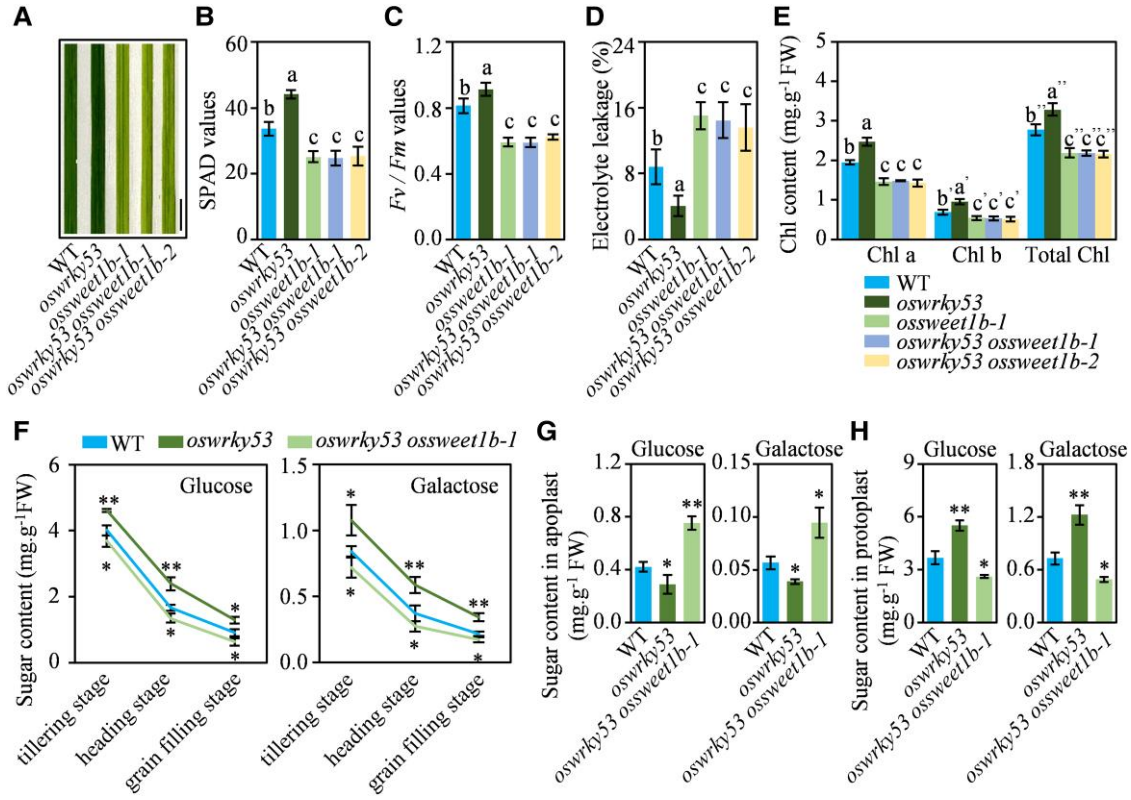

Figure 8. *OsWRKY53* genetically acts upstream of *OsSWEET1b*. **A)** Leaf phenotype of *oswrky53*, *ossweet1b*, and *oswrky53 osweet1b* mutants at the heading stage. Scale bar: 1 cm. **B)** SPAD values of flag leaf of *oswrky53*, *ossweet1b*, and *oswrky53 osweet1b* mutants at the heading stage. **C)** Fv/Fm values of flag leaf of *oswrky53*, *ossweet1b*, and *oswrky53 osweet1b* mutants at the heading stage. **D)** Electrolyte leakage analysis of flag leaf of *oswrky53*, *ossweet1b*, and *oswrky53 osweet1b* mutants at the heading stage. **E)** Chlorophyll content of flag leaf of *oswrky53*, *ossweet1b*, and *oswrky53 osweet1b* mutants at the heading stage. **F)** Glucose and galactose contents in flag leaf of the *oswrky53* and *oswrky53 osweet1b* mutants at the different growth stages. **G)** Apoplastic sugar contents in the *oswrky53* and *oswrky53 osweet1b* mutants at 3-wk-old seedling stage. **H)** Sugar contents in protoplasts of the *oswrky53* and *oswrky53 osweet1b* mutants at 3-wk-old seedling stage. Data represent mean ± SE of 3 biological replicates. The different letters above each bar in **B)**, **C)**, **D)**, and **E)** indicate statistically significant differences, as determined by 1-way ANOVA analysis followed by Tukey's multiple test ($P < 0.05$). Asterisks in **F)**, **G)**, and **H)** indicate a significant difference between transgenic plants and WT as determined by 2-tailed Student's *t* test at $^{**}P < 0.01$ or $^{*}P < 0.05$.

growth stages. From the tillering stage to heading stage and grain filling stage, higher contents of glucose and galactose were observed in the *oswrky53* mutant, while lower levels of these 2 sugars were calculated in the *OsWRKY53*-OE plant relative to them in the WT (Supplementary Fig. S10). However, contents of fructose, mannose, and sucrose were comparable between the *OsWRKY53*-OE plant or *oswrky53* mutant and WT (Supplementary Fig. S10). Since both the *ossweet1b* mutant and the *OsWRKY53*-OE plant accumulated less glucose and galactose, and all showed accelerated leaf senescence, we thus analyzed response of the *OsWRKY53*-OE plant to exogenous application of sugar under dark treatment to validate whether the accelerated leaf senescence of *OsWRKY53*-OE plant was sugar dependent. After dark incubation, the *OsWRKY53*-OE leaf discs showed severely yellowish, accompanying with decreased chlorophyll contents, activated *OsI57* expression, and suppressed *OsDOS* expression than those in the WT (Supplementary Fig. S11). Exogenous applications of glucose and galactose could substantially delay the senescence under dark treatment in the *OsWRKY53*-OE plant and WT, as evidenced by the higher chlorophyll contents compared with mock-treated plants. However, both glucose and galactose application could delay the senescence of the *OsWRKY53*-OE plant that the transgenic plants even showed higher chlorophyll contents than mock-treated WT (Supplementary Fig. S11). In agreement, the *OsWRKY53*-OE plant had lower *OsI57* expression and higher *OsDOS* expression after treatment of glucose or galactose than mock-treated WT (Supplementary Fig. S11). Collectively, these results support that OsWRKY53 genetically acts upstream of *OsSWEET1b* by regulating glucose and galactose import to modulate leaf senescence.

OsSWEET1b-mediated sugar import promotes agronomic traits

To investigate the effect of OsSWEET1b-mediated sugar import on rice growth and development, we planted the *OsSWEET1b*-OE plant and *ossweet1b* mutant in the paddy field along with WT and examined a set of agronomic traits

of them. The *ossweet1b* mutants showed decreased plant height (−15%∼20%), tiller number (−43%∼52%), grain width (−9%∼11%), seed setting rate (−44%∼54%), panicle length (−16%∼18%), grain number per panicle (−50%∼54%), and 1,000-grain weight (−28% ∼ 32%) than the WT. Reversely, the *OsSWEET1b*-OE plants had increased panicle length (+5%∼10%) and grain number per panicle (+10%∼17%) than the WT, while no significant differences in plant height, tiller number, grain width, seed setting rate, and 1,000-grain weight were observed between the *OsSWEET1b*-OE plant and WT (Supplementary Fig. S12), suggesting that *OsSWEET1b* has positive effect on grain-related traits.

Discussion

Sugars are primary respiratory substrates in plant cells. However, along with natural leaf senescence, attenuated nutrient translocation such as insufficient sugars transportation from older leaves to young leaves can cause sugar starvation which accelerates the process (Kim 2019; Woo et al. 2019). Here, we reported that senescence-activated transcription factor OsWRKY53 suppresses the expression of *OsSWEET1b*, leading to deficient sugar accumulation in leaf cells where sugar starvation promotes leaf senescence.

Accumulating evidence shows that SWEETs largely prefer to transport sugars, such as sucrose, glucose, galactose, fructose, and mannose (Xue et al. 2022). It has been shown that 6 rice OsSWEETs can transport glucose and OsSWEET5 can transport galactose when tested in yeast or *Xenopus* oocytes (Xue et al. 2022). In this study, we demonstrate that OsSWEET1b harbors influx transport activity for glucose and galactose. The substantial evidence to support the conclusion is that (i) OsSWEET1b could transport glucose and galactose while not other sugars when tested in *Xenopus* oocytes using ^{14}C-labeled sugars as substrates (Fig. 4), (ii) OsSWEET1b had influx transport activity but not efflux transport activity toward glucose and galactose when heterologously expressed in *Xenopus* oocytes (Fig. 4), (iii) loss-of-function of *OsSWEET1b* in planta could significantly decrease glucose and galactose accumulation in leaf cells (Fig. 5), and (iv) exogenous application of glucose and galactose could complement the defect of loss-of-function of *OsSWEET1b*-caused accelerated leaf senescence (Fig. 6). The biochemical and physiological assays together confirm that OsSWEET1b is a sugar importer.

SWEET-mediated sugar transportation alters sugar homeostasis in leaf cells which influences leaf senescence. Sugar starvation is positively associated with the process of leaf senescence that has been reported for overexpressing of sugar exporters AtSWEET11, AtSWEET12, and AtSWEET15 in Arabidopsis and PbSWEET4 in strawberry or deletion of sugar importer ZmSWEET1b in maize (Seo et al. 2011; Eom et al. 2015; Chen, Cheung, et al. 2015; Chen, Lin, et al. 2015; Ni et al. 2020; Wu et al. 2023). Our data support that OsSWEET1b acts as a sugar importer translocating glucose and galactose from the extracellular apoplast into the intracellular cytosol. Glucose and galactose could not be sufficiently transported into cytosol, resulting in sugar starvation in the *ossweet1b* mutants (Fig. 5). In line with previously reported that SWEET-mediated sugar starvation promotes leaf senescence, the *ossweet1b* mutants showed accelerated leaf senescence compared with delayed leaf senescence of the *OsSWEET1b*-OE plants (Fig. 1). Interestingly, both OsSWEET5 and OsSWEET1b could transport galactose testing in yeast; however, the *OsSWEET5*-overexpressing transgenic plants and the *ossweet1b* mutants had a similar precocious senescence phenotype. We suppose the conflict between these 2 rice SWEETs may be caused by their different sugar transport activity or ability as they belong to different SWEET family clades (Yuan et al. 2014). ZmSWEET1b is an ortholog of OsSWEET1b. The *zmsweet1b* knockout mutants accumulated less sucrose and fructose and had a senescence phenotype (Wu et al. 2023). We infer that OsSWEET1b and ZmSWEET1b might experience divergent selection during rice and maize evolution; thus, they may employ different sugars as their substrates. Moreover, senescence processes are largely linked to energy reutilization in plants; sugars have been suggested as the key signaling molecules that influence the progression of leaf senescence. Sugar sensors are proposed to sense exogenous sugars involved in signal transduction to delay senescence (Kim 2019). Moreover, numerous studies have reported that low sugar levels could accelerate senescence responses; supplementing sugars in developmentally senescing leaves could suppress or delay the senescence responses (Wingler et al. 2009; Kim 2019; Li et al. 2020). Rice Hxk1 is involved in hexose-sensing process at the early stage of leaf senescence (Li et al. 2020). OsSWEET4, OsSWEET5, and OsSWEET15 could transport galactose in yeast (Yuan et al. 2014; Tao et al. 2015); OsSWEET14 is an influx transporter for glucose (Chen et al. 2012). Whether Hxk1 or these SWEET proteins play roles in reverting the senescence for *ossweet1b* mutants is unclear. In addition, several plant SWEETs have also been shown to be involved in the movement of phytohormones, such as Arabidopsis AtSWEET13 and AtSWEET14, and rice OsSWEET3a could mediate cellular GA uptake (Kanno et al. 2016; Morii et al. 2020), and barley (*Hordeum vulgare*) HvSWEET11b could transport cytokinin (Radchuk et al. 2023). Although OsSWEET1b could not uptake GA in yeast (Morii et al. 2020), whether it can transport GA or cytokinin in planta is unclear, since GA and cytokinin are senescence inhibitors (Woo et al. 2019). Therefore, we could not rule out the possibility that OsSWEET1b might also transport GA or cytokinin to influence the progression of senescence.

Previously, we found that *OsWRKY53* participates in ABA-induced leaf senescence (Tian et al. 2017; Xie et al. 2022), and it has an opposite expressional pattern compared with *OsSWEET1b* in leaf along with natural leaf senescence (Yuan et al. 2014; Xie et al. 2022). Here, we update the underlying molecular mechanism for OsWRKY53-regulated leaf senescence that OsWRKY53 directly targets *OsSWEET1b* to

alter sugar homeostasis to influence senescence, which is supported by the following evidence: (i) the *OsSWEET1b* expression was significantly increased in the *oswrky53* mutant while decreased in the *OsWRKY53*-overexpressing plants (Fig. 7A), (ii) the direct bind of OsWRKY53 to the promoter of *OsSWEET1b* was validated by EMSA and ChIP assays (Fig. 7), (iii) suppression of OsWRKY53 on *OsSWEET1b* expression was confirmed by transient expression assay (Fig. 7D), (iv) knocking out of *OsSWEET1b* in the *oswrky53* mutant could impair the delayed senescence phenotype of *oswrky53* mutant (Fig. 8), (v) there were comparable glucose and galactose contents in flag leaf of the *oswrky53* mutant and the *OsSWEET1b*-OE plants or the *ossweet1b* mutant and the *OsWRKY53*-overexpressing plants (Figs. 5 and 8), and (vi) exogenous applications of glucose and galactose could comparably decelerate the senescence of both the *ossweet1b* mutant and the *OsWRKY53*-overexpressing plants (Fig. 6). These biochemical, genetic, and physiological assays synthetically confirm that *OsWRKY53*-regulated *OsSWEET1b* module is involved in leaf senescence. Moreover, we previously showed that *OsWRKY53* regulates leaf senescence by enhancing ABA accumulation (Xie et al. 2022). Thus, published results and present data demonstrate that OsWRKY53 regulates different downstream target genes to alter ABA and sugar signaling pathways to modulate leaf senescence (Fig. 9). There are complex interactions between ABA and sugar modulating the onset or progress of leaf senescence (Wingler and Roitsch 2008). Although the *OsSWEET1b* transgenic plants had similar expression of ABA biosynthetic genes and comparable ABA content compared with WT (Supplementary Fig. S13), whether there is crosstalk between ABA and sugar in OsWRKY53-regulated leaf senescence should be deciphered further. In addition, a number of hormone-related biosynthetic or metabolic genes have altered expression levels in the *OsWRKY53* transgenic plant leaves (Chujo et al. 2014; Xie et al. 2021, 2022). Therefore, functioning as a transcriptional repressor, OsWRKY53 may also target other genes or alter other hormone homeostasis to regulate leaf senescence. The corresponding target genes and the underlying mechanism are waiting for uncovering.

Sugars, acting as the main supervisor and key sources of energy, are involved in general development of plants from the stage of embryogenesis to senescence. Evidence supports a role of sugar starvation in the initiation and/or acceleration of leaf senescence (Kim 2019; Woo et al. 2019; Li et al. 2020). Moreover, intercellular and intracellular sugars have long been considered to act as important signal molecules that can generally affect fundamental cellular processes including senescence or regulate gene expression during leaf senescence (Wingler et al. 2009; Asim et al. 2023). Knocking out of *OsSWEET1b* caused glucose and galactose retention in the extracellular apoplast, resulting in sugar starvation in the intracellular cytosol. We conjectured that sugar starvation-caused energy shortage and sugar starvation-initiated senescence signal might accelerate leaf senescence in the *ossweet1b* mutant, which should be verified in the future. Moreover, the high K_m value for OsSWEET1b suggests that OsSWEET1b is a low-affinity transporter and it has influx activity in a pretty high amount of sugars. In line with that, the *ossweet1b* mutants exhibiting substantially accelerated senescence from the tillering stage to the senescence stage may reflect that OsSWEET1b functions mainly at the corresponding stages when rice plants accumulate abundant sugars (Kim 2019). However, whether other rice SWEET members have synergistic or antagonistic effects along with OsSWEET1b in the process of sugar starvation-promoted leaf senescence might be explored, especially at the stages when leaves accumulate a large amount of sugars.

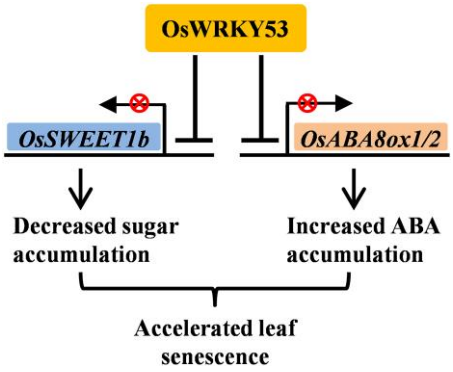

Figure 9. Proposed working model of OsWRKY53-regulated senescence. OsWRKY53 binds and suppresses the expressions of *OsSWEET1b* and *OsABA8ox1* or *OsABA8ox2*, causing decreased sugar accumulation and increased ABA accumulation in leaf cells, respectively. The attenuated sugar content and enhanced ABA level coordinately promote leaf senescence.

Delaying the progress of leaf senescence has been associated with improved crop yields and utilized as an alternative breeding strategy (Thomas and Ougham 2014). It is worth noting that both the *OsSWEET1b*-OE plants and the *oswrky53* mutants had delayed the progress of leaf senescence and increased grain-related traits (Tian et al. 2017; Xie et al. 2021, 2022). Thus, modulating the expressions of *OsWRKY53* or *OsSWEET1b* might be an applicable strategy for genetic improvement.

In summary, our findings verify that OsSWEET1b acts as a sugar transporter capable of translocating glucose and galactose from the extracellular apoplast into the intracellular cytosol. The senescence-activated transcription factor OsWRKY53 directly binds to the promoter of *OsSWEET1b* and suppresses its expression, leading to compromised glucose and galactose accumulation in leaf cells where sugar starvation accelerates leaf senescence.

Materials and methods

Plant materials and growth conditions

The *OsWRKY53*-OE and *OsWRKY53*:GFP plants and *oswrky53* and *ossweet1b* knockout mutants were generated previously in rice (*O. sativa* ssp. *Geng*) cultivar 'Zhonghua 11' (ZH11)

background (Xie et al. 2021; Li et al. 2022). The *OsSWEET1b*-OE transgenic lines were generated in ZH11 as described below. The *oswrky53 ossweet1b* double mutants were generated by deleting *OsSWEET1b* in the *oswrky53* mutant. The seeds were sown on the seedbed, and 1 mo later, germinated seedlings were transplanted to the paddy field in the experimental station on campus. All rice materials were planted in regular growing season from May to October with field management and fertilizer application as described previously (Chu et al. 2022).

Plant treatments

The dark-induced leaf senescence experiments were performed as described previously (Xie et al. 2022). In brief, the transgenic rice lines and WT were planted in soil and grown 1 mo in a controlled environment plant growth chamber under a 14 h light/10 h dark cycle at 28 °C. Detached leaves were cut into 1 cm pieces, immersed in 2 mM MES solution at pH 5.7, and incubated in complete darkness for 5 d. Rice plants at the tillering stage were inoculation with bacterial pathogens *Xanthomonas oryzae* pv. *oryzae* strain PXO99 and *X. oryzae* pv. *oryzicola* strain RH3 and fungal pathogen *Magnaporthe oryzae* isolate 99-20-2 and were sampled at the designated times as described previously (Tian et al. 2023). Seedlings at the 4-leaf stage were treated with drought (stopping the water supply), salt (irrigation with 200 mM NaCl solution), and cold (4 °C growth chamber) and were sampled at the designated times as described previously (Lv et al. 2017). The calli of ZH11 were treated with sugars (incubation with 100 mM glucose or galactose) and sampled for a certain period of time.

Chlorophyll measurement

Rice leaves from the transgenic rice lines and WT at different growth stages were sampled for chlorophyll measurement (Xie et al. 2022). About 100 mg samples were incubated in extraction solution (absolute ethanol:acetone:water, 4.5:4.5:1, *v*/*v*/*v*) for 12 h; then, the extraction was measured spectrophotometrically at 645 and 663 nm using a Spark Multimode Microplate Reader (Tecan, Switzerland). Total chlorophyll (mg/g) = $(20.29A_{645} + 8.05A_{663}) \times v/m \times 1{,}000$, where v is the volume of extraction solution and m is the mass of leaves.

SPAD and Fv/Fm measurement

The uppermost fully expanded leaf from the transgenic rice lines and WT growing in the paddy field at the tillering stage, heading stage, and grain filling stage was marked for SPAD and Fv/Fm measurement (Tian et al. 2023). A chlorophyll SPAD-502 meter was used to assess SPAD value that 3 SPAD readings per leaf were taken around the midpoint and again 40 mm away on both sides of the midpoint. The OS30p$^+$ Chlorophyll Fluorometer was used to measure Fv/Fm value. SPAD reading and Fv/Fm value for each plot was determined by taking the average of 30 readings.

Ion leakage rate measurement

The detached leaves were cut into 1 cm piece and submerged in 10 mL of deionized water in test tubes for 12 h at room temperature. A DDSJ-308A conductivity meter was used for measuring the initial conductivity (R1). Then, the test tubes were placed in boiling water for 30 min and naturally cooled to room temperature; the conductivity (R2) was measured again. The R1/R2 was calculated as ion leakage rate (Xie et al. 2022).

Sugar influx and efflux activity in *Xenopus* oocytes

Transport activity of OsSWEET1b was determined as previously reported (Chen et al. 2012; Wang et al. 2022). In brief, cRNA was prepared by T7 polymerase using the mMESSAGE mMACHINE kit. Fifty nanoliters of cRNA or RNase-free water was injected into each oocyte. For sugar influx assay, 2 d after injection, 8 oocytes were transferred into tubes containing 200 μL of Na-Ringer buffer (2 mM KCl, 115 mM NaCl, 1.8 mM $CaCl_2$, 1 mM $MgCl_2$, and 10 mM HEPES-Tris, pH 7.5) with 100 mg/L gentamycin and 100 μM sucrose (4 μCi/mL [^{14}C]sucrose), glucose (4 μCi/mL [^{14}C]glucose), or galactose (4 μCi/mL [^{14}C]galactose). After incubation 2 h at 18 °C, the oocytes were washed with cold sucrose in Na-Ringer buffer 3 times and then extracted by 0.1 M HNO_3, and the radioactivity was calculated by a liquid scintillation analyzer. For sugar efflux assay, 2 d after cRNA injection, oocytes were further injected with 50 nL of solution containing 1 mM sucrose (0.15 μCi/mL [^{14}C]sucrose), glucose (0.15 μCi/mL [^{14}C]glucose), or galactose (0.15 μCi/mL [^{14}C]galactose). Eight oocytes per replicate were transformed into tubes and immediately washed with cold Na-Ringer buffer 3 times. The cells were then incubated in 500 μL of Na-Ringer buffer, and the external buffer was collected at 0.5 and 2 h. The radioactivity of external solution and oocytes was determined by a liquid scintillation analyzer. The efflux activity was expressed as a percentage [radioactivity in external solution/(radioactivity in external solution + radioactivity remaining in the oocytes) × 100].

Measurement of sugar and starch contents

Rice flag leaves from the transgenic rice lines and WT at the tillering stage, heading stage, and grain filling stage were sampled for sugar and starch measurement. About 200 mg samples were ground in liquid nitrogen and extracted with a solution of 1.6 mL methanol:chloroform:water (5:2:2, *v*/*v*/*v*) via incubation for 30 min at 70 °C. After ultrasound treatment for 90 min, the samples were centrifuged at 4,000 rpm for 10 min; then, the supernatant was collected and mixed with 200 μL of methyl-α-D-glucopyranoside as an internal standard. After centrifugation at 12,000 rpm for 15 min, 0.5 mL of supernatant were collected and dried in a vacuum concentrator at 60 °C. The dried metabolites were orderly derivatized with hydroxylamine hydrochloride, hexamethyl disilylamine, and trimethylchlorosilane and transferred to glass vials for Q Exactive Plus Hybrid Quadrupole-Orbitrap Mass Spectrometer

(ThermoFisher Scientific, United States) analysis with the parameters as reported previously (Li et al. 2022). Leaves of 3-wk-old rice seedlings were harvested for apoplastic fluid extraction. Apoplastic fluid extraction was performed as described previously (Nouchi et al. 2012). In brief, leaves were cut in small fragments and soaked in a surfactant solution containing 0.05% (*v*/*v*) Triton X-100 for 2 min. After rinsing with deionized water, fragments were infiltrated using a 60 mL syringe with a 3-way stopcock for 3 min. The syringe was then set in a sealant injector with the inner pressure of the syringe kept at maximum pressurization for 5 min. Then, the leaf fragments were inserted into a centrifuge tube and centrifuged at 6,000 × *g* for 15 min at 4 °C. The apoplastic fluid flowed out from the leaf fragments and collected at the bottom of the centrifuge tube using a micropipette. Rice protoplasts were isolated using 3-wk-old seedlings as described previously (Xie et al. 2021). The starch content in flag leaf was extracted via the DMSO/HCl method and measured enzymatically using a starch assay kit according to the manufacturer's instruction (Megazyme, Bray, Ireland).

Gene expression analysis

The TRIzol reagent (Invitrogen, United States) was used to isolate total RNA from various rice tissues at different growth stages when rice plants ZH11 were grown in a paddy field. The mRNA was reverse-transcribed into cDNAs using MonScript RTIII All-in-One Mix (Monad, China) according to the manufacturer's protocol. qPCR was performed using MonAmp SYBR Green qPCR Mix (Monad, China) in the ABI QuantStudio (Applied Biosystems, United States). Gene-specific primers were designed using primer analysis software Primer Express v3.0 (Applied Biosystems, United States). Transcript level of rice *actin* gene was used to normalize expression level for target genes (Supplementary Table S2). Each RT-qPCR assay was performed with 3 independent biological replicates, with each repetition having 3 technical replicates. The differences were analyzed for statistical significance using 2-tailed Student's *t* test.

Yeast 1-hybrid assay

The Matchmaker Gold Yeast One-Hybrid System (Clontech, United States) was used for screening putative transcription factors binding to *OsSWEET1b* promoter. A 2 kb *OsSWEET1b* promoter upstream of the initiation codon of *OsSWEET1b* gene was cloned into pAbAi vector and transformed into the gold strain (Y1HGold) to generate a bait-reporter yeast. The yeast strain was then transformed with the pGAD424-based rice leaf cDNA library. Transformants were spread on SD/-Leu medium, and positive colonies were picked for plasmid extraction.

ChIP-qPCR

The ChIP assays were conducted as described previously. In brief, chromatin was extracted from the *OsWRKY53:GFP* seedlings (Xie et al. 2021) and fragmented to 200 to 400 bp via ultrasound. The OsWRKY53:GFP protein bonding DNAs were enriched by protein A Dynabeads (Invitrogen, United States) coupling with anti-GFP antibody or IgG as control at 4 °C overnight. After extensive washing and decrosslinking, the input and precipitated DNA samples were amplified by qPCR using gene-specific primers (Supplementary Table S2).

Recombinant protein production

The coding sequence of *OsWRKY53* was amplified and cloned into the pCold vector using the gene-specific primers (Supplementary Table S2). Both the recombinant plasmid and control plasmid were transformed into *Escherichia coli* BL21(DE3) cells; then, cells were induced with 0.2 mM isopropyl β-D-1-thiogalactopyranoside (IPTG) overnight at 16 °C and collected by centrifugation (Xie et al. 2021). The recombinant His-TF-OsWRKY53 protein and control His-TF protein were purified using Ni Sepharose 6 fast Flow (GE Healthcare, United States).

EMSA

EMSA assays were conducted using LightShift Chemiluminescent EMSA Kit (Thermo Scientific, United States) as described previously (Xie et al. 2021). In brief, the 5-carboxyfluorescein (FAM) biotin-labeled probes were synthesized and incubated with purified His-TF-OsWRKY53 recombinant proteins for 30 min at room temperature. The unlabeled probes were mixed with labeled probes for competition reaction. The mutant probes were used as negative control. The protein–DNA complex was separated on a 6% (*v*/*v*) PAGE gel for 2 h at 4 °C in the dark. Gels were photographed using FLA-5100 (FUJIFILM, Japan).

Transient expression assays in rice protoplasts

OsSWEET1b promoter (2 kb upstream of the translational ATG start codon) was amplified by PCR using gene-specific primers (Supplementary Table S2) and then cloned into the pGreen II 0800 vector to generate the $P_{OsSWEET1b}$:LUC construct as reporter. Moreover, the $mP_{OsSWEET1b}$:LUC construct was generated by mutating the 2 W-box motifs (−1,048∼−1,043 and −194∼−189 bp) from TTGACC to TTCGGC using the GeneTailor Site-Directed Mutagenesis System (Invitrogen Life Technologies, United States) at the *OsSWEET1b* promoter. The coding sequence of *OsWRKY53* was amplified with gene-specific primers (Supplementary Table S2) and cloned into the pU1301 vector to generate the Ubi:OsWRKY53 construct as effector. The reporter and effector constructs were cotransfected into rice protoplasts as described previously (Xie et al. 2021). After culturing in the dark for 16 h at 25 °C, the transfected protoplasts were collected by centrifugation at 100 × *g* for 8 min. The LUC activities were measured by a Spark Multimode Microplate Reader (Tecan, Switzerland) using Dual Luciferase Reporter Assay System (Promega, United States) according to the manufacturer's instructions. The relative reporter gene expression levels were expressed as the ratio of firefly LUC to renilla luciferase (REN).

Subcellular localization assay

OsSWEET1b full-length cDNA without the translational stop codon was amplified using the specific primers (Supplementary Table S2); then, the amplified PCR products were inserted into the pM999-GFP vector between the *Kpn*I and *BamH*I restriction sites (Yang et al. 2022), to generate the OsSWEET1b:GFP construct where *OsSWEET1b* was in-frame and upstream of the green fluorescent protein (*GFP*) that was driven by the CaMV 35S promoter. The OsSWEET1b:GFP construct was transiently transformed into rice protoplasts isolated from 20-d-old green rice leaf sheaths via polyethylene glycol (PEG)-mediated transient protoplast transformation (Yang et al. 2022). The protoplasts were incubated at 28 °C for 12 h and then were visualized for fluorescent signals by a Leica Microsystem (LAS AF, Germany) with GFP excited at 488 nm and detected at 500 to 530 nm according to a previously reported protocol (Yang et al. 2022).

DAB staining

Rice plants were grown in the paddy field till to the grain filling stage; flag leaf was sampled and used for DAB staining according to previously described protocol (Chu et al. 2022). In brief, DAB was dissolved in a buffer containing 10 mM 2-(N-morpholinol)ethanesulfonic acid and 0.2% (*v*/*v*) Tween 20 to a final concentration of 1 mg/mL. Leaves were vacuum-infiltrated with DAB solution for 12 h in the dark and then immersed in ethanol to remove chlorophyll in a water bath at 60 °C overnight.

Histochemical experiments

Flag leaf of rice plants at the grain filling stage were sampled and immediately frozen in liquid nitrogen. The contents of hydrogen peroxide (H_2O_2), SOD, POD, and MDA were measured using assay kits (Elabscience, United States), according to the manufacturer's instructions. All the measurements were biologically repeated with 3 times.

Statistical analysis

Statistical parameters are represented in the figures and figure legends. The differences between samples were analyzed for statistical significance using Student's *t* test or ANOVA.

Accession numbers

Sequence data from this article can be found in the Rice Genome Annotation Project (RGAP) data libraries under the following accession numbers: *OsSWEET1b* (LOC_Os05g35140), *OsWRKY53* (LOC_Os05g27730), *OsDOS* (LOC_Os01g09620), *OsI57* (LOC_Os02g57260), and *OsI85* (LOC_Os07g34520).

Acknowledgments

We are grateful to Professor Shaowu Xue at Huazhong Agricultural University for assistance in *Xenopus* oocytes assays.

Author contributions

M.Y. designed the research. D.C. and Y.S. performed most of the experiments. W.X., P.Z., S.L., and J.X. assisted the experiments. M.Y. and D.C. analyzed the data and drafted the manuscript. M.Y. wrote and revised the manuscript.

Supplementary data

The following materials are available in the online version of this article.

Supplementary Figure S1. Relative transcript levels for *OsSWEET1b* in the *OsSWEET1b*-OE transgenic lines.

Supplementary Figure S2. Phenotype of *OsSWEET1b*-OE, *ossweet1b*, and WT at the different growth stages.

Supplementary Figure S3. Temporal changes of chlorophyll levels in the flag leaf of *OsSWEET1b*-OE, *ossweet1b*, and WT at the different growth stages.

Supplementary Figure S4. Knockout of *OsSWEET1b* promotes dark-induced senescence.

Supplementary Figure S5. Expression pattern of *OsSWEET1b*.

Supplementary Figure S6. Altered starch contents and transcript levels of starch synthesis genes in flag leaf of *OsSWEET1b* transgenic plants.

Supplementary Figure S7. Exogenous applications of sucrose and fructose did not delay the accelerated leaf senescence of *ossweet1b* mutant.

Supplementary Figure S8. Binding activity of OsWRKY53 on the W-box motif by EMSA.

Supplementary Figure S9. Characterization of the *oswrky53 ossweet1b* double mutant.

Supplementary Figure S10. Sugar contents in flag leaf of the *oswrky53* mutant and *OsWRKY53*-OE plant at different growth stages.

Supplementary Figure S11. Exogenous applications of glucose and galactose delayed the accelerated leaf senescence of *OsWRKY53*-OE plants.

Supplementary Figure S12. Agronomic traits in grains of the *ossweet1b* mutant and *OsSWEET1b-OE* plant grown in field.

Supplementary Figure S13. Transcript levels of ABA biosynthetic genes and ABA contents in flag leaf of *OsSWEET1b* transgenic plants.

Supplementary Table S1. Putative transcription factors associated with *OsSWEET1b* promoter.

Supplementary Table S2. Primers used in this study.

Funding

This work was supported by grants from the National Natural Science Foundation of China (31821005 and 32172421), the Major Project of Hubei Hongshan Laboratory (2022hszd016), the Natural Science Foundation of Hubei Province (2023AFA043), and the Fundamental Research Funds for the Central Universities (2662023PY006).

Conflict of interest statement. None declared.

References

Asim M, Zhang Y, Sun Y, Guo M, Khan R, Wang XL, Hussain Q, Shi Y. Leaf senescence attributes: the novel and emerging role of sugars as signaling molecules and the overlap of sugars and hormones signaling nodes. Crit Rev Biotechnol. 2023:**43**:1092–1110. https://doi.org/10.1080/07388551.2022.2094215

Burdiak P, Mielecki J, Gawroński P, Karpiński S. The CRK5 and WRKY53 are conditional regulators of senescence and stomatal conductance in *Arabidopsis*. Cells 2022:**11**(22):3558. https://doi.org/10.3390/cells11223558

Chen LQ, Cheung LS, Feng L, Tanner W, Frommer WB. Transport of sugars. Annu Rev Biochem. 2015:**84**(1):865–894. https://doi.org/10.1146/annurev-biochem-060614-033904

Chen LQ, Lin IW, Qu XQ, Sosso D, McFarlane HE, Londoño A, Samuels AL, Frommer WB. A cascade of sequentially expressed sucrose transporters in the seed coat and endosperm provides nutrition for the *Arabidopsis* embryo. Plant Cell. 2015:**27**(3):607–619. https://doi.org/10.1105/tpc.114.134585

Chen LQ, Qu XQ, Hou BH, Sosso D, Osorio S, Fernie AR, Frommer WB. Sucrose efflux mediated by SWEET proteins as a key step for phloem transport. Science 2012:**335**(6065):207–211. https://doi.org/10.1126/science.1213351

Chu C, Huang R, Liu L, Tang G, Xiao J, Yoo H, Yuan M. The rice heavy-metal transporter OsNRAMP1 regulates disease resistance by modulating ROS homoeostasis. Plant Cell Environ. 2022:**45**(4):1109–1126. https://doi.org/10.1111/pce.14263

Chujo T, Miyamoto K, Ogawa S, Masuda Y, Shimizu T, Kishi-Kaboshi M, Takahashi A, Nishizawa Y, Minami E, Nojiri H, et al. Overexpression of phosphomimic mutated OsWRKY53 leads to enhanced blast resistance in rice. PLoS One 2014:**9**(6):e98737. https://doi.org/10.1371/journal.pone.0098737

Eom JS, Chen LQ, Sosso D, Julius BT, Lin IW, Qu XQ, Braun DM, Frommer WB. SWEETs, transporters for intracellular and intercellular sugar translocation. Curr Opin Plant Biol. 2015:**25**:53–62. https://doi.org/10.1016/j.pbi.2015.04.005

Han M, Kim CY, Lee J, Lee SK, Jeon JS. OsWRKY42 represses *OsMT1d* and induces reactive oxygen species and leaf senescence in rice. Mol Cells. 2014:**37**(7):532–539. https://doi.org/10.14348/molcells.2014.0128

Jiang H, Li M, Liang N, Yan H, Wei Y, Xu X, Liu J, Xu Z, Chen F, Wu G. Molecular cloning and function analysis of the stay green gene in rice. Plant J. 2007:**52**(2):197–209. https://doi.org/10.1111/j.1365-313X.2007.03221.x

Kanno Y, Oikawa T, Chiba Y, Ishimaru Y, Shimizu T, Sano N, Koshiba T, Kamiya Y, Ueda M, Seo M. AtSWEET13 and AtSWEET14 regulate gibberellin-mediated physiological processes. Nat Commun. 2016:**7**(1):13245. https://doi.org/10.1038/ncomms13245

Kim J. Sugar metabolism as input signals and fuel for leaf senescence. Genes Genomics. 2019:**41**(7):737–746. https://doi.org/10.1007/s13258-019-00804-y

Kong Z, Li M, Yang W, Xu W, Xue Y. A novel nuclear-localized CCCH-type zinc finger protein, OsDOS, is involved in delaying leaf senescence in rice. Plant Physiol. 2006:**141**(4):1376–1388. https://doi.org/10.1104/pp.106.082941

Lee RH, Wang CH, Huang LT, Chen SC. Leaf senescence in rice plants: cloning and characterization of senescence up-regulated genes. J Exp Bot. 2001:**52**(358):1117–1121. https://doi.org/10.1093/jexbot/52.358.1117

Li P, Wang L, Wang S, Yuan M. Impaired *SWEET*-mediated sugar transportation impacts starch metabolism in developing rice seeds. Crop J. 2022:**10**(1):98–108. https://doi.org/10.1016/j.cj.2021.04.012

Li Z, Zhao Q, Cheng F. Sugar starvation enhances leaf senescence and gene involved in sugar signaling pathways regulate early leaf senescence in mutant rice. Rice Sci. 2020:**27**(3):201–214. https://doi.org/10.1016/j.rsci.2019.11.001

Lv Y, Yang M, Hu D, Yang Z, Ma S, Li X, Xiong L. The OsMYB30 transcription factor suppresses cold tolerance by interacting with a JAZ protein and suppressing β-amylase expression. Plant Physiol. 2017:**173**(2):1475–1491. https://doi.org/10.1104/pp.16.01725

Morii M, Sugihara A, Takehara S, Kanno Y, Kawai K, Hobo T, Hattori M, Yoshimura H, Seo M, Ueguchi-Tanaka M. The dual function of OsSWEET3a as a gibberellin and glucose transporter is important for young shoot development in rice. Plant Cell Physiol. 2020:**61**(11):1935–1945. https://doi.org/10.1093/pcp/pcaa130

Ni J, Li J, Zhu R, Zhang M, Qi K, Zhang S, Wu J. Overexpression of sugar transporter gene *PbSWEET4* of pear causes sugar reduce and early senescence in leaves. Gene 2020:**743**:144582. https://doi.org/10.1016/j.gene.2020.144582

Nouchi I, Hayashi K, Hiradate S, Ishikawa S, Fukuoka M, Chen CP, Kobayashi K. Overcoming the difficulties in collecting apoplastic fluid from rice leaves by the infiltration-centrifugation method. Plant Cell Physiol. 2012:**53**(9):1659–1668. https://doi.org/10.1093/pcp/pcs102

Ohdan T, Francisco PB Jr, Sawada T, Hirose T, Terao T, Satoh H, Nakamura Y. Expression profiling of genes involved in starch synthesis in sink and source organs of rice. J Exp Bot. 2005:**56**(422):3229–3244. https://doi.org/10.1093/jxb/eri292

Radchuk V, Belew ZM, Gündel A, Mayer S, Hilo A, Hensel G, SharmaR, Neumann K, Ortleb S, Wagner S, et al. SWEET11b transports both sugar and cytokinin in developing barley grains. Plant Cell. 2023:**35**(6):2186–2207. https://doi.org/10.1093/plcell/koad055

Robatzek S, Somssich IE. Targets of AtWRKY6 regulation during plant senescence and pathogen defense. Genes Dev. 2002:**16**(9):1139–1149. https://doi.org/10.1101/gad.222702

Sato Y, Morita R, Katsuma S, Nishimura M, Tanaka A, Kusaba M. Two short-chain dehydrogenase/reductases, NON-YELLOW COLORING 1 and NYC1-LIKE, are required for chlorophyll b and light-harvesting complex II degradation during senescence in rice. Plant J. 2009:**57**(1):120–131. https://doi.org/10.1111/j.1365-313X.2008.03670.x

Seo PJ, Park JM, Kang SK, Kim SG, Park CM. An *Arabidopsis* senescence-associated protein SAG29 regulates cell viability under high salinity. Planta 2011:**233**(1):189–200. https://doi.org/10.1007/s00425-010-1293-8

Tang Y, Li M, Chen Y, Wu P, Wu G, Jiang H. Knockdown of *OsPAO* and *OsRCCR1* cause different plant death phenotypes in rice. J Plant Physiol. 2011:**168**(16):1952–1959. https://doi.org/10.1016/j.jplph.2011.05.026

Tao Y, Cheung LS, Li S, Eom JS, Chen LQ, Xu Y, Perry K, Frommer WB, Feng L. Structure of a eukaryotic SWEET transporter in a homotrimeric complex. Nature 2015:**527**(7577):259–263. https://doi.org/10.1038/nature15391

Thomas H, Ougham H. The stay-green trait. J Exp Bot. 2014:**65**(14):3889–3900. https://doi.org/10.1093/jxb/eru037

Tian X, Li X, Zhou W, Ren Y, Wang Z, Liu Z, Tang J, Tong H, Fang J, Bu Q. Transcription factor OsWRKY53 positively regulates brassinosteroid signaling and plant architecture. Plant Physiol. 2017:**175**(3):1337–1349. https://doi.org/10.1104/pp.17.00946

Tian J, Wang L, Hui S, Yang D, He Y, Yuan M. Cadmium accumulation regulated by a rice heavy-metal importer is harmful for host plant and leaf bacteria. J Adv Res. 2023:**45**:43–57. https://doi.org/10.1016/j.jare.2022.05.010

van Doorn WG. Is the onset of senescence in leaf cells of intact plants due to low or high sugar levels? J Exp Bot. 2008:**59**(8):1963–1972. https://doi.org/10.1093/jxb/ern076

Wang H, Chen W, Xu Z, Chen M, Yu D. Functions of WRKYs in plant growth and development. Trends Plant Sci. 2023:**28**(6):630–645. https://doi.org/10.1016/j.tplants.2022.12.012

Wang J, Yu YC, Li Y, Chen LQ. Hexose transporter SWEET5 confers galactose sensitivity to Arabidopsis pollen germination via a galactokinase. Plant Physiol. 2022:**189**(1):388–401. https://doi.org/10.1093/plphys/kiac068

Wang P, Gao J, Wan C, Zhang F, Xu Z, Huang X, Sun X, Deng X. Divinyl chlorophyll(ide) a can be converted to monovinyl chlorophyll(ide) a by a divinyl reductase in rice. Plant Physiol. 2010:**153**(3):994–1003. https://doi.org/10.1104/pp.110.158477

Wang Y, Cui X, Yang B, Xu S, Wei X, Zhao P, Niu F, Sun M, Wang C, Cheng H, et al. Ranscription factor positively regulates leaf senescence and the defense response by modulating the transcription of genes implicated in the biosynthesis of reactive oxygen species and salicylic acid in *Arabidopsis*. Development 2020:**147**:dev189647. https://doi.org/10.1242/dev.189647

Wingler A, Masclaux-Daubresse C, Fischer AM. Sugars, senescence, and ageing in plants and heterotrophic organisms. J Exp Bot. 2009:**60**(4):1063–1066. https://doi.org/10.1093/jxb/erp067

Wingler A, Roitsch T. Metabolic regulation of leaf senescence: interactions of sugar signalling with biotic and abiotic stress responses. Plant Biol. 2008:**10**(s1):50–62. https://doi.org/10.1111/j.1438-8677.2008.00086.x

Woo HR, Kim HJ, Lim PO, Nam HG. Leaf senescence: systems and dynamics aspects. Annu Rev Plant Biol. 2019:**70**(1):347–376. https://doi.org/10.1146/annurev-arplant-050718-095859

Wu Y, Wang S, Du W, Ding Y, Li W, Chen Y, Zheng Z, Wang Y. Sugar transporter ZmSWEET1b is responsible for assimilate allocation and salt stress response in maize. Funct Integr Genomics. 2023:**23**(2):137. https://doi.org/10.1007/s10142-023-01062-8

Xie W, Ke Y, Cao J, Wang S, Yuan M. Knock out of transcription factor WRKY53 thickens sclerenchyma cell walls, confers bacterial blight resistance. Plant Physiol. 2021:**187**(3):1746–1761. https://doi.org/10.1093/plphys/kiab400

Xie W, Li X, Wang S, Yuan M. *OsWRKY53* promotes abscisic acid accumulation to accelerate leaf senescence and inhibit seed germination by downregulating abscisic acid catabolic genes in rice. Front Plant Sci. 2022:**12**:816156. https://doi.org/10.3389/fpls.2021.816156

Xue X, Wang J, Shukla D, Cheung LS, Chen LQ. When SWEETs turn tweens: updates and perspectives. Annu Rev Plant Biol. 2022:**73**(1):379–403. https://doi.org/10.1146/annurev-arplant-070621-093907

Yang Z, Hui S, Lv Y, Zhang M, Chen D, Tian J, Zhang H, Liu H, Cao J, Xie W, et al. miR395-regulated sulfate metabolism exploits pathogen sensitivity to sulfate to boost immunity in rice. Mol Plant. 2022:**15**(4):671–688. https://doi.org/10.1016/j.molp.2021.12.013

Yu Y, Qi Y, Xu J, Dai X, Chen J, Dong CH, Xiang F. Arabidopsis WRKY71 regulates ethylene-mediated leaf senescence by directly activating *EIN2*, *ORE1* and *ACS2* genes. Plant J. 2021:**107**(6):1819–1836. https://doi.org/10.1111/tpj.15433

Yuan M, Zhao J, Huang R, Li X, Xiao J, Wang S. Rice MtN3/saliva/SWEET gene family: evolution, expression profiling, and sugar transport. J Integr Plant Biol. 2014:**56**(6):559–570. https://doi.org/10.1111/jipb.12173

Zeng ZQ, Lin TZ, Zhao JY, Zheng TH, Xu LF, Wang YH, Liu LL, Jiang L, Chen SH, Wan JM. *Oshema* gene, encoding glutamyl-tRNA reductase (GluTR) is essential for chlorophyll biosynthesis in rice (*Oryza sativa*). J Integr Agr. 2020:**19**(3):612–623. https://doi.org/10.1016/S2095-3119(19)62710-3

Zhang H, Li J, Yoo JH, Yoo SC, Cho SH, Koh HJ, Seo HS, Paek NC. Rice Chlorina-1 and Chlorina-9 encode ChlD and ChlI subunits of Mg-chelatase, a key enzyme for chlorophyll synthesis and chloroplast development. Plant Mol Biol. 2006:**62**(3):325–337. https://doi.org/10.1007/s11103-006-9024-z

Zhang Y, Liu Z, Wang X, Wang J, Fan K, Li Z, Lin W. DELLA proteins negatively regulate dark-induced senescence and chlorophyll degradation in *Arabidopsis* through interaction with the transcription factor WRKY6. Plant Cell Rep. 2018:**37**(7):981–992. https://doi.org/10.1007/s00299-018-2282-9

Zhou Y, Liu L, Huang W, Yuan M, Zhou F, Li X, Lin Y. Overexpression of *OsSWEET5* in rice causes growth retardation and precocious senescence. PLoS One 2014:**9**(4):e94210. https://doi.org/10.1371/journal.pone.0094210